Integration and simulation of a bitumen upgrading facility and an IGCC process with carbon capture

By
Gemayel El Gemayel

Thesis submitted to the Faculty of Graduate and Postdoctoral Studies
in partial fulfillment of the requirements for the
M.A.Sc. degree in Chemical Engineering

Department of Chemical and Biological Engineering
University of Ottawa
August 2012

Statement of Contribution of Collaborators

I am the sole author of all the chapters of this thesis. My supervisors, Dr. Arturo Macchi of the Department of Chemical and Biological Engineering, University of Ottawa, and Dr. Edward John Anthony of CanmetENERGY, Natural Resources Canada, supervised my work during the M.A.Sc. program and provided editorial corrections.

Abstract

Hydrocracking and hydrotreating are bitumen upgrading technologies designed to enhance fuel quality by decreasing its density, viscosity, boiling point and heteroatom content via hydrogen addition. The aim of this thesis is to model and simulate an upgrading and integrated gasification combined cycle then to evaluate the feasibility of integrating slurry hydrocracking, trickle-bed hydrotreating and residue gasification using the Aspen HYSYS® simulation software.

The close-coupling of the bitumen upgrading facilities with gasification should lead to a hydrogen, steam and power self-sufficient upgrading facility with CO_2 capture. Hydrocracker residue is first withdrawn from a 100,000 BPD Athabasca bitumen upgrading facility, characterized via ultimate analysis and then fed to a gasification unit where it produces hydrogen that is partially recycled to the hydrocracker and hydrotreaters and partially burned for power production in a high hydrogen combined cycle unit. The integrated design is simulated for a base case of 90% carbon capture utilizing a monoethanolamine (MEA) solvent, and compared to 65% and no carbon capture scenarios.

The hydrogen production of the gasification process is evaluated in terms of hydrocracker residue and auxiliary petroleum coke feeds. The power production is determined for various carbon capture cases and for an optimal hydrocracking operation. Hence, the feasibility of the integration of the upgrading process and the IGCC resides in meeting the hydrogen demand of the upgrading facility while producing enough steam and electricity for a power and energy self-sufficient operation, regardless of the extent of carbon capture.

Sommaire

L’hydrocraquage et l'hydrotraitement sont des technologies d’amélioration du pétrole brut, conçues pour augmenter la qualité d’un carburant en diminuant sa densité, sa viscosité, son point d'ébullition et son contenu en hétéroatome, grâce à l’addition d'hydrogène. L'objectif de cette thèse est de modéliser et de simuler un procédé d’amélioration de bitume et un cycle combiné à gazéification intégrée afin d’évaluer la faisabilité d’intégrer l’hydrocraquage dans une colonne à bulles, l'hydrotraitement dans des lits fixes et la gazéification de résidus en utilisant le logiciel de simulation Aspen HYSYS®.

La combinaison du procédé d’amélioration du bitume avec la technologie de gazéification devrait permettre l’autosuffisance en hydrogène, en vapeur et en électricité tout en permettant la séquestration du dioxyde de carbone. Le résidu d'hydrocraquage est retiré du procédé d’amélioration de 100,000 barils de bitume d’Athabasca par jour et caractérisé par «analyse ultime» pour ensuite être alimentée à une unité de gazéification. De plus, le procédé est simulé afin d’assurer une séquestration du dioxyde de carbone de 90% et 65% en utilisant un solvant de monoéthanolamine (MEA).

La production d'hydrogène du procédé de gazéification est évaluée par rapport à une co-alimentation de coke de pétrole et de résidus d'hydrocraquage. La production d'électricité est évaluée pour divers cas de séquestration du dioxyde de carbone et pour une opération d'hydrocraquage optimale. Conséquemment, la faisabilité de l'intégration des procédés d’amélioration du bitume et de gazéification est justifiée par une production nécessaire d'hydrogène, permettant l’alimentation soutenue de l’hydrocraqueur et des hydrotraiteurs, tout en maintenant l’autosuffisance du procédé en énergie et en électricité, quelle que soit l'étendue de la séquestration du dioxyde de carbone.

Acknowledgments

I wish to express my sincere gratitude to my co-supervisors, Arturo Macchi and E.J. ‘Ben’ Anthony for their invaluable assistance, guidance and support. I am also deeply indebted to Robin Hughes for his helpful advice and for the time he has given me throughout my Master’s thesis.

My special thanks to David McCalden and Dennis Lu from CanmetENERGY Bells Corner Complex for their involvement in the team meetings and their expert input on the gasification process. I would like to take this opportunity to thank Edward Little, Jinwen Chen and Mugurel Munteanu for allowing me to cooperate with CanmetENERGY Devon and having the privilege to work alongside their very dynamic and enthusiastic research group. The cooperation between the CanmetENERGY Ottawa and Devon facilities has allowed me to benefit from valuable research and industrial expertise in gasification and heavy oil upgrading. I also want to recognize Theo de Bruijn for proposing the novel idea of integrating the Canmet slurry hydrocracker with a gasification process.

Finally, I wish to avail myself of this opportunity to express my sense of gratitude to my dearly loved parents and brother, for their perpetual assistance and affection and to my friends for being by my side and supporting me throughout my endeavours.

Table of contents

List of Tables

List of Figures

Nomenclature List

α_i = Mass fraction distribution parameter of species “i"

β = Hydrogen partial pressure exponential parameter

ε = Gas phase hold-up

E_A = Activation energy (J/mol)

γ_i = Heteroatom distribution parameter of species “i"

k_A = Forward reaction rate constant ($MPa^{\beta}.h^{-1}$)

k_{A0} = Pre-exponential factor (h^{-1})

LE_{Ci} = Light end carbon number distribution from “i" = 1 to 4

M = Molecular weight (g/mol)

η_i = Mass fraction of species “i" (kg of A/ kg total)

η_{i0} = Inlet mass fraction of species “i" (kg of A/ kg total)

ρ_A = Density of species A (kg/m^3)

P_{H2} = Hydrogen partial pressure (MPa)

R = Gas constant (J/[K.mol])

r_A = Reaction rate of species A ($kg/m^3/h$)

$Ratio\frac{HDN}{HDS}$ = Ratio of hydrodenitrogenation to hydrodesulfurization conversion

SG = Specific gravity

T = Temperature (K)

T_b = Boiling point temperature (K)

V = Reactor volume (m^3)

v_{AB0} = Total volumetric flow rate (m^3/h)

X = Residue conversion

X_{HDS} = Hydrodesulfurization conversion

X_{HDN} = Hydrodenitrogenation conversion

Acronym list

ASU = Air separation unit

AGR = Acid gas removal

BPD = Barrels per day

CCR = Conradson carbon residue

GT = Gas turbine

HGO = Heavy gas oil

HHV = Higher heating value

HP = High pressure

HPS = High pressure steam

IGCC = Integrated gasification combined cycle

IP = Intermediate pressure

LE = Light ends

LGO = Light gas oil

LP = Low Pressure

MEA = Monoethanolamine

MP = Medium pressure

NPH = Naphtha

PFD = Process flow diagram

RCR = Ramsbottom carbon residue

SARA = Saturates aromatics resins asphaltenes

SCO = Synthetic crude oil

TBP = True boiling point

VR = Vacuum residue

WGS = Water-gas shift

1. Introduction

1.1. General introduction

The initiative of improving the living conditions of today's society, the industrialization of many underdeveloped countries and the increase in world population are some of the reasons causing a rise in worldwide energy demand. Countries not belonging to the Organization for Economic Co-operation and Development (OECD), such as India and China, are forecasted to be responsible for 93% of the increase in global energy demand between 2007 and 2030. Fossil fuels will account for 77% of the increase in world primary energy demand during those years. The oil demand is predicted to climb from 85 to 105 Mbbl per day [1]. Unconventional oils resources consisting mainly of heavy oils and bitumen are estimated at 6×10^{12} barrels. However, their impact on today's global petroleum market is still marginal [2]. It is therefore essential to study and improve the efficiency of the bitumen upgrading facilities in order to meet future energy demands and effectively contribute to the world energy market.

Bitumen is a mixture of heavy hydrocarbons with a low heating value and a high heteroatom content, boiling point, density and viscosity. In order to increase its value, the bitumen is upgraded to lighter and more valuable petroleum fractions via carbon rejection or hydrogen addition. The carbon rejection procedure which represents 56.6% of the total worldwide processing capacity consists of reducing the carbon percentage in the oil product via thermally cracking [2, 3]. This leads to the formation of a solid amalgamated carbonaceous by-product called "coke" that can be removed from the treated product. An increase in coking conversion tends to produce lighter petroleum fractions, to the detriment of the product's mass yield [3-11]. Delayed and fluid coking, fluid catalytic cracking and visbreaking are examples of available carbon rejection upgrading technologies. Conversely, hydrogen addition is the other upgrading method and the one simulated in this thesis. The technology consists of breaking and/or adding hydrogen to the heavy oil hydrocarbons, in a hydrogen rich environment. The procedure increases the hydrogen percentage of the heavy oil while effectively reducing its carbon to hydrogen ratio and avoiding the production of coke. Hydrocracking, hydrotreating and hydroconversion are common upgrading technologies operated in today's petroleum industry [4, 8].

First discovered in Germany around 1915, hydrocracking is one of the oldest petroleum conversion processes. It was applied in the field of coal conversion in order to optimize the production of liquid fuels and gained importance in Germany during World War II. The impact of hydrocracking diminished greatly after 1945 because of the Middle Eastern domination of the petroleum market which removed the incentive to convert coal or unconventional oils to liquid fuels [4]. The technology reflourished around 1960 when processes like the "Isocracking process" by the Chevron Research Company, "Unicracking-JHC" by Unocal-ESSO and "Lomax" by Universal Oil Products (UOP) were developed [3]. Since then, hydrocracking became widely used for the upgrading of bitumen and heavy oils.

Even though hydrocracking is an upgrading technology that is a century old, most of the significantly funded research is proprietary. Very little accurate public literature is available. The selection of the most selective catalysts and accurate hydrocracking kinetics are available usually after pilot or demonstration-scale testing which are expensive and generated on contractual terms. Public information on hydrocracker models generally omit hydrocarbon and hydrogen mass transfer limitations, catalyst deactivation and effects of hydrogen partial pressure on reaction conversion [12-24].

Bitumen upgrading plants utilizing hydrogen addition technologies require a large amount of hydrogen, generally produced on-site. Globally, about 96% of this hydrogen is generated via natural gas and light naphtha steam reforming. Partial oxidation of residues like petroleum coke, deasphalter pitch and vacuum residue, i.e. gasification, consist of the remaining 4% (see Table 1.1) [25]. If combined with an upgrading facility, partial oxidation can however be advantageous since it gives the attractive feature of gasifying its highly carbonaceous pitch so as to contribute to its hydrogen demand.

Table 1.1: Worldwide energy consumption (Quadrillion BTU) and percentage occupied by fossil fuels [26]

	2005	2006	2007	2008	2009
Petroleum	170.10	170.80	171.80	172.30	169.90
Natural gas	103.19	105.99	109.53	113.17	108.80
Coal	122.55	127.05	132.78	138.83	137.34
Total energy	458.69	468.28	478.45	490.84	482.97

	2005	2006	2007	2008	2009
Petroleum	37.08%	36.47%	35.91%	35.10%	35.18%
Natural gas	22.50%	22.63%	22.89%	23.06%	22.53%
Coal	26.72%	27.13%	27.75%	28.28%	28.44%
Total fossil fuels	86.30%	86.24%	86.55%	86.44%	86.14%

CanmetENERGY proposes integrating the residue of an upgrading process utilizing the Canmet slurry hydrocracker with entrained flow slagging gasifier (see Figure 1.1). This innovative combination can lead to self-sustainability with regards to the plant's net hydrogen and electrical consumption. The Canmet slurry hydrocracker also requires the addition of a fine iron-based powder which reduces the hydroprocessing coking yield while successively decreasing the gasifier's operating temperature due to the iron's favorable influence on the slag rheology [27, 28]. Moreover, since environmental regulations are becoming more stringent, the close coupling of both processes can reduce the heteroatom content in the synthetic crude oil (SCO) while allowing near-zero sulfur and metals tail gas emissions. Carbon sequestration technologies are also included in the upgrading process in order to control CO_2 emissions.

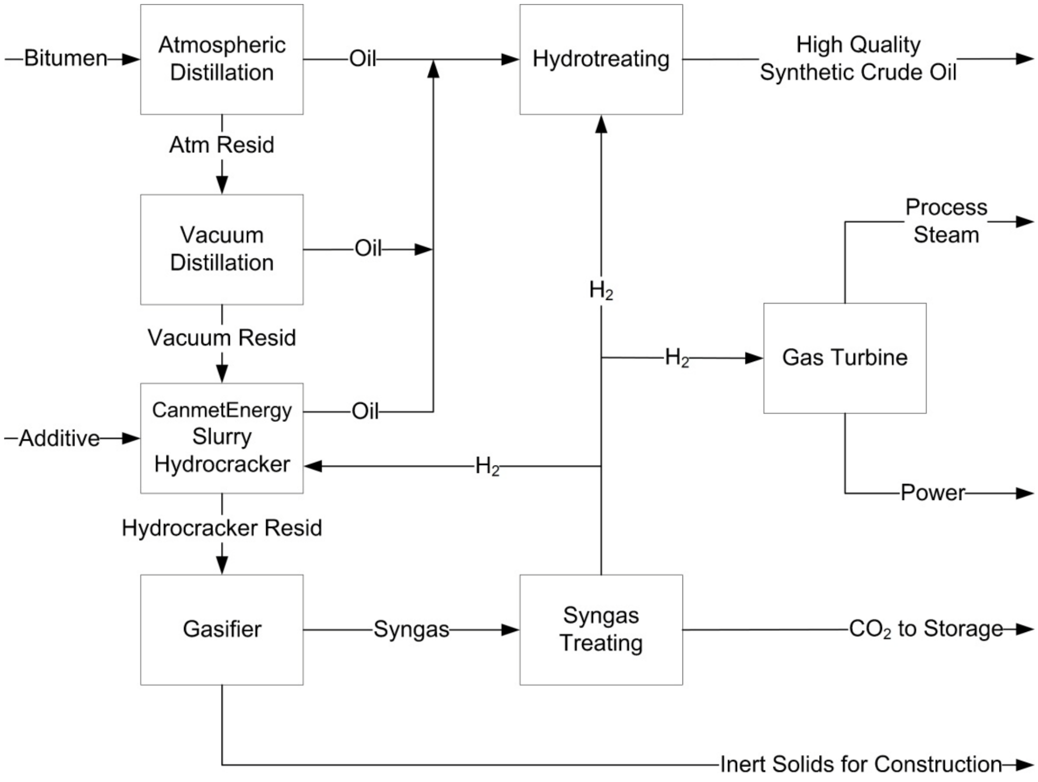

Figure 1.1: Simplified block flow diagram of the upgrading and gasification integrated process

A few industrial plants integrating bitumen upgrading and gasification are available worldwide. The Long Lake integrated bitumen and upgrading project is the first large-scale gasification operation operated in conjunction with a heavy-oil upgrading process in Canada [29]. North West Upgrading is collaborating with Linde in order to integrate their upgrading process with the

Linde MPG technology [30]. Shell's Pernis refinery in Rotterdam incorporated their refinery with a gasification unit that processes visbreaker residue or straight-run vacuum residue [31]. Moreover, other plants like Suncor's Millennium coker, CNRL Horizon and Petro-Canada Sturgeon Upgrader are promoting the integration of coking and thermal upgrading technologies with gasification for hydrogen production [32].

1.2. ***Thesis objectives***

The purpose of this thesis is study the technical feasibility of combining a bitumen upgrading facility with an Integrated Gasification Combined Cycle (IGCC) process. The upgrading process requires the modeling of a Canmet slurry hydrocracker with the characterization and calibration of distillation towers and hydrotreating reactors. The IGCC process on the other hand consists of an Air Separation Unit (ASU), an entrained flow slagging gasifier, an Acid Gas Removal (AGR) section, a Water-Gas Shift (WGS) reactors in series, a CO_2 compression cycle, a sulfur recovery unit, a high hydrogen power generation combined cycle. The goal of the upgrading facility is to produce a quality Synthetic Crude Oil (SCO) with a density of around 30ºAPI and a heteroatom content below 1wt% sulfur and 0.1wt% nitrogen while calculating the required hydrogen demand of the upgrading units. The hydrocracker residue is extracted and charged into a gasification process resulting in hydrogen production. The integrated design is simulated for the case of 90%, 65% and 0% carbon capture, utilizing a monoethanolamine (MEA) solvent. A hydrocracker residue and coke co-feed is added to the process in order to increase hydrogen, steam and power production while keeping the heteroatom content in the flue gas below environmental regulatory limits. Ultimately, the benefit of close-coupling the bitumen upgrading facilities with gasification resides in achieving a hydrogen and power self-sufficient upgrading facility with CO_2 capture while producing a high yield of SCO with low heteroatom content.

During the subsequent chapters, the simulation software utilized for the integration of the Canmet Slurry Hydrocracking upgrading process and the Integrated Gasification Combined Cycle is validated (chapter 3). The simulation's Process Flow Diagram (PFD) is then presented and detailed (chapter 4). Every major unit operation is described in accordance with their operating conditions and key specifications. The optimization work and case studies associated with the simulation are then presented in two sequential articles (chapters 5 and 6); the upgrading simulation's results are exhibited in the first paper whereas the integrated bitumen upgrading process and gasification simulation is detailed in the sequel. The overall simulation's results and conclusions are finally discussed, accompanied by recommendations regarding future simulation expansion work (chapter 7).

2. Petroleum specifications and process simulation description

The origin of oil

Petroleum is believed to have originated from the decay of flora and fauna in an oxygen-free environment [10]. The accumulation of the carbon based life-form in the bottom of oceans and river deltas, at high pressure, followed by a coating of sand, shells, bones and rocks eventually led to the formation of liquid hydrocarbons. The buildup of oil eventually settling between nonporous rocks led to the creation of reservoirs. The heteroatom content of the oil was contingent on the amount of inorganic sulfur, metal complexes and salt water that contacted the organic matter. The oil composition also depended on the nature and location where it matured. Marine petroleum has the tendency to be less paraffinic and more naphthenic and aromatic than terrestrial deposits. Reservoirs might also have been subject to thermal cracking depending on the depths of their burial and the reservoir temperature. Heavier oils were formed when petroleum reservoirs leaked, allowing the oil to flow to oxygen-rich environments where microorganisms consume the lighter paraffinic petroleum fraction while leaving behind heavier oil deposits such as the oil sands of northern Alberta, Canada [11]. Studies around the world showed that petroleum is subject to biodegradation when present at depths less than 600 meters and temperatures below 80ºC [33].

2.1. ***Bitumen characterization***

Bitumen is a dense, viscous and high boiling point mixture of hydrocarbons that has an elevated average carbon number, aromaticity and heteroatom content. The complex bitumen mixture cannot be easily modeled due to the different variety of present molecules without a reoccurring molecular structure. Therefore, petroleum mixtures are generally simplified via characterization techniques. Separating the bitumen in True Boiling Point (TBP) cuts [12, 15-23] which lumps the hydrocarbons present in the petroleum mixture based on their boiling points or performing a SARA (saturates, aromatics, resins and asphaltenes) analysis [34] are common characterization techniques utilized in the petroleum industry to typify intricate oil mixtures.

2.1.1. Boiling point categorization

Boiling point distribution

Boiling point distribution characterization can consist of a discrete lumping approach and a continuum theory of lumping. The discrete lumping approach is a type of petroleum characterization that is based on popular lumps defined in the petroleum industry such as naphtha and diesel. The cuts act as pseudo-components which contain all molecules present in the boiling point range it characterizes. To increase the precision of a system, the amount of lumps can be augmented which results in a more refined, yet intricate, representation of the hydrocarbon mixture. This characterization method allows for a more manageable approach to petroleum processing like approximating distillation product flow rates or hydrocracking reaction paths (see Figure 2.1) [22, 35].

Fraction	TBP (°C)
Naphtha + Gases	< 180
Diesel	180 – 380
Gas Oil	380 – 540
Vacuum Residue	> 540

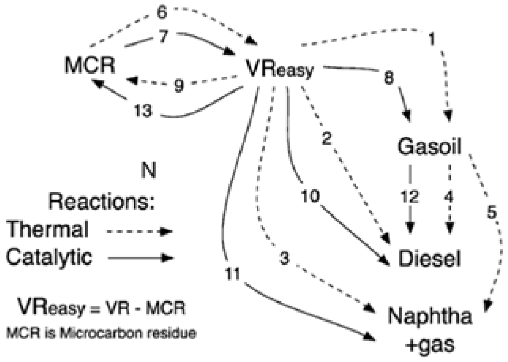

Figure 2.1: Boiling point ranges of some petroleum fractions and their proposed reaction paths [10, 35]

The continuum theory of lumping on the other hand is a characterization method that considers bitumen as a continuous mixture with respect to its boiling point. It is normalized with regards to its True Boiling Point (TBP), allowing the mixture to have a continuous boiling point that ranges from the most volatile to the heaviest molecule in the mixture [23]. The continuous lumping approach is therefore a distribution from 0 to 1 of the simulated distillation curve (see Figure 2.2).

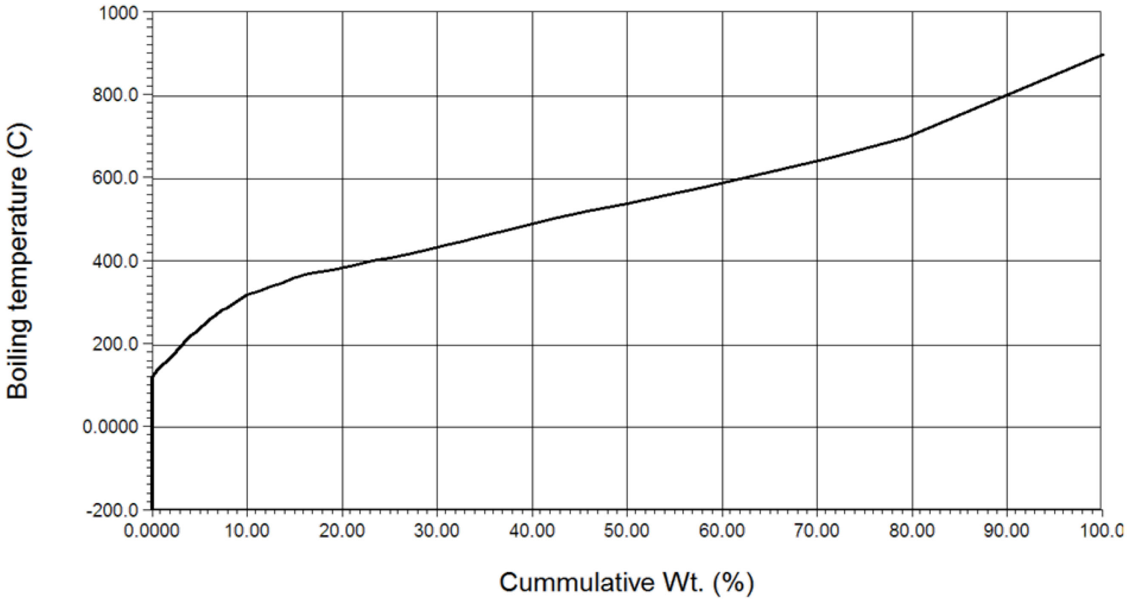

Figure 2.2: TBP simulated distillation curve of bitumen

SARA analysis

The SARA analysis is a technique that divides crude depending on its polarity and carbon structure. Saturates consist mainly of aliphatic compounds, aromatics include mainly mono and polycyclic aromatic hydrocarbons, resins constitute essentially of heterocyclic (Nitrogen, Oxygen and Sulfur) compounds such as acids, bases, phenolic and naturally occurring compounds and asphaltene consists of connected cyclic and aromatic molecules [34].

The benefit of a SARA analysis is the capability to track asphaltenes which are a concentrated lump of molecules that are prone to be converted into coke at high temperatures. The SARA analysis can assist in depicting the heavy oil quality by summarizing the general content of a petroleum sample [36].

2.1.2. Bitumen properties

Density and API Gravity

Raw bitumen is a dense petroleum fraction that is around 1000 kg/m^3. One of the objectives of upgrading bitumen is to reduce the density of the oil, a property that is also function of molecular weight, hydrogen content and heteroatom content [8]. Furthermore, small density variations have a considerable effect on the fuel quality and value. Therefore, the petroleum industry utilizes ºAPI (see equation 2.1), a more sensitive measuring scale that is inversely proportional to the density of crude. Generally, the API gravity of a heavy oil fraction rises with its value [10].

$$\text{ºAPI} = \frac{141.5}{\text{specific gravity at 60ºF (15.6ºC)}} - 131.5 \qquad 2.1$$

When dealing with a pseudo-component, all the properties are assumed constant and are calculated or measured at the average Normal Boiling Point (NBP) or the Final Boiling Point (FBP) of the cut [5]. Similarly to the boiling point distribution discussed earlier

Molecular weight

Determining the molecular weight of a bitumen fraction gives an insight about the cut's density and boiling point. A petroleum fraction with a higher molecular weight than another indicates that it might also have a higher density and boiling point. The bitumen's molecular weight can range from an average of 3,000 to over 10,000 [3, 8, 10].

$$\mathrm{M} = 42.965\ \mathrm{T_b^{1.26007}}\ \mathrm{SG^{4.98308}} \exp\begin{bmatrix} 2.097 * 10^{-4}\ \mathrm{T_b} - 7.78712\ \mathrm{SG} \\ +2.08476 * 10^{-3}\ \mathrm{T_b}\ \mathrm{SG} \end{bmatrix} \qquad 2.2$$

The average molecular weight of a petroleum cut is found via freezing point depression osmometry or gel permeation chromatography [5], but if not specified, correlations like equation 2.2 can estimate the molecular weight as a function of boiling point (T_b) and specific gravity (SG) [37].

Viscosity

Viscosity is a property that dictates the flowability and transportability of a certain liquid. During the extraction, upgrading and refining of heavy oils, the viscosity of the petroleum fraction affects the process design parameters. The oil rheology can be estimated in function of its boiling point, density and molecular weight, but can greatly differ from the actual value when dealing with heavy oils and bitumen. As a result, the viscosity can also be measured at 100ºF (37.8ºC) and 210ºF (99ºC) from a variety of ASTM tests if more accurate results are required [5]. Simulation software can have different viscosity correlations depending on the boiling point of crude but heavier fractions are correlated in Aspen simulators by Twu's kinetic viscosity correlation which has an average error of around 8.53% for boiling points up to 727ºC [38].

At room temperature, bitumen has a viscosity that can exceed 300,000 cP. This is why heavier petroleum fuels with higher density and boiling point are either heated or mixed with a lighter fraction like naphtha before pumping.

Carbon residue

The carbon residue content is the petroleum portion that is likely to deposit as coke under severe thermal conditions (e.g., 500ºC), affecting the process engineering design parameters [8]. Determined with methods like the Ramsbottom (RCR) or Conradson (CCR) ASTM tests, bitumen tends to have higher carbon residue content than petroleum crude hence lowering its value [7].

Heteroatom content

A heteroatom is any atom that is not a carbon and hydrogen. In liquid petroleum, the presence of sulfur, nitrogen, metals and salts influences the downstream upgrading process and might require further upgrading in order to remove the heteroatoms for environmental purposes [10]. The sulfur content and density of a crude are two properties that have the greatest effect on the value of the crude [8]. A crude oil is generally considered sour when its sulfur content exceeds 0.5wt%. Canadian bitumen is very dense and high in sulfur hence it is much less valuable than sweet crude from countries such as Saudi Arabia. Similarly, crude oil nitrogen contents exceeding 0.25% are undesirable due to catalyst poisoning and corrosion effects caused downstream. Moreover, SO_X and NO_X are hazardous compounds produced when igniting fuels with high sulfur and nitrogen contents, which is why their composition is strictly controlled by environmental regulations [39]. The petroleum metal content can have substantial corrosion, fouling and environmental impacts regardless of their concentration [40]. Small quantities of nickel or vanadium can cause significant catalyst fouling in catalytic petroleum upgrading units and severe equipment corrosion [41]. The metal content is generally highest in the vacuum residue wherein the organometallic compounds can be extracted with the use of a solvent [7]. If the heavy fraction undergoes coking, the metals can also be mainly removed with the produced coke [42].

2.2. Simulation software

The software selected for the simulation of the bitumen upgrading facility and the IGCC process is Aspen HYSYS$^{®}$, a program that has established itself as a market-leading process modeling tool that is frequently used in the petroleum upgrading and refining industry by companies like Petrobras, Preem and PTT [43]. The program contains a user friendly graphical user interface (GUI) that is ideal for building, customizing and combining large simulations. Aspen HYSYS$^{®}$ also authorizes user variables, model customizations and software extensions to VBA, aspenOne, Microsoft Excel, etc. [44, 45] The software is equipped with a strong thermodynamic foundation with a variety of property packages and the option to modify or interact with externally constructed thermodynamic packages [46, 47]. Containing over 1,000 pure components, Aspen HYSYS$^{®}$ has the option to create hypothetical compounds and assist the user in defining crude oil assays in its Oil Environment where oil properties and characteristics can be specified or estimated with several embedded correlations. Aspen HYSYS Refining (formerly called RefSYS) is an extra licensed package that allows a user to modify or import various petroleum assays. A petroleum assay is a laboratory chemical evaluation of a petroleum crude oil. Assay properties contain values of density, viscosity, molecular weight, sulfur content, etc. The refining package also includes specific upgrading and refinery unit operations that can be calibrated in order to model various design specifications [48].

The operation of Aspen HYSYS$^{®}$ is based on the interaction between two program environments. The components, thermodynamic package, reactions, petroleum assay and hypothetical compounds are defined in the Basis Environment. Also, when additions or modifications are made in the Basis Environment, the simulation is put on hold in order to maintain peak efficiency and avoid unnecessary and conflicting flowsheet calculations [48]. The Simulation Environment is a flowsheet that is always linked to the Basis Environment in which the defined simulation components are interacting in the various unit operations that are offered.

2.3. Aspen HYSYS® feed characterization

2.3.1. Bitumen feed

The Aspen HYSYS® characterization of crude oil is executed in the simulator Oil Environment where a petroleum assay is primarily defined by its boiling point distribution, density, molecular weight, viscosity, and light end composition. The entered data helps generate hypothetical pseudo-components that characterize the defined crude assay. The software generates and displays a simulated distillation curve allowing the user to visually verify the characterized petroleum fraction (see Figure 2.2). Oil properties are estimated with various embedded correlations if they are not available experimentally. However, it is advised to thoroughly characterize the feed with experimental data in order to better define the system [44]. The additional Aspen HYSYS Refining license permits the user to individually vary the property of each pseudo-component, allowing characteristics like the heteroatom content, the aromatic content, the density, the molecular weight, the viscosity and the C to H ratio to be changed for individual components [48].

2.3.2. Hydrocracker residue

The gasifier is a unit in which carbonaceous fuels of different qualities are converted to gaseous products of higher heating value. Each gasification design has to be customized in order to avoid fouling, scaling or any type of damage that can be potentially inflicted by fuel impurities, on the process units [49]. Over 95% of the liquid feedstocks gasified worldwide consist of refinery residues with different densities, viscosities, heteroatom content, C to H ratios and SARA analysis, e.g. atmospheric, vacuum and hydrocracker residue or asphalts. When the gasifier operating parameters are kept constant, the various feedstocks yield a product gas with different CO/H_2 ratios [50].

The C to H ratio on a mass basis can vary from 7 to 10 for vacuum residues. Although that difference affects the composition of CO and H_2 in the gasifier product, the parameter is not involved in determining the heteroatom content of the syngas. The sulfur and nitrogen content in the feedstock are the atoms that influence the production rate of noxious molecules like H_2S, NH_3, HCN, COS and CS_2 which have to be removed downstream. A high metal and ash content affects the viscosity of the slag and might also necessitate removal if entrained with the syngas. The viscosities, pour point, flash point and Conradson carbon content are other important parameters that are considered during the design of the pretreatment units, i.e. pumping and heating, of the gasification feedstock [50, 51].

During the integration of the bitumen upgrading section with the IGCC, it is necessary to establish the elemental analysis of the gasifier feedstock. Since petroleum assays are represented in Aspen HYSYS® as an array of hypothetical pseudo-components with different boiling points, their conversion into elementary form is necessary in order to mimic the reaction dynamics of the high temperature system and allow the simulation program to accurately represent the petroleum fraction as a gasifier feed. If the Higher Heating Value (HHV) of stream elemental analysis is different than the original petroleum feedstock, the addition of energy to the system is required in order to avoid discrepancies in the overall energy balance [52-55].

An elemental analysis is constructed by initially determining the sulfur, nitrogen and oxygen content of the petroleum fraction. The sulfur and nitrogen compositions are calculated by Aspen HYSYS® based on the bitumen heteroatom distribution. The carbon and hydrogen percentages are assigned based on the C to H ratio of the assay, a value that is estimated in the Aspen HYSYS® simulator using a mass blend approach [48]. Unfortunately, if the estimated C to H bulk value is inconsistent with public literature data [8], then an experimentally found C to H ratio has to be used in order to represent the case with more accuracy [56].

2.3.3. Synthetic Crude Oil

The naphtha (NPH), light gas oil (LGO) and heavy gas oil (HGO) blend is called Synthetic Crude Oil following a reduction in metal, asphaltenes, CCR and heteroatoms (sulfur and nitrogen) content [4]. The typical SCO properties are shown in Table 2.1. Moreover, it is sent for further refining (hydrocracking or fluid catalytic cracking) in order to produce marketable petroleum fuel products.

Table 2.1: Athabasca SCO properties [57]

API Gravity (ºAPI)	27.71
Kinematic viscosity (mm2/s)	4.66 @ 40ºC
	2.11 @ 80ºC
Freezing point (ºC)	< -60
Carbon Residue (wt%)	0.0028
Sulfur content (wt%)	0.136
Nitrogen content (wt%)	0.079

2.4. Plant overview

Two different processes are simulated and combined in Aspen HYSYS®. The proposed petroleum upgrading plant is simulated with a feed of 100,000 bbl/day of Athabasca bitumen (see Figure 2.3) that undergoes an atmospheric and vacuum distillation in order to separate the original petroleum mixture into light ends, naphtha (NPH), light gas oil (LGO), heavy gas oil (HGO) and vacuum residue. The NPH, LGO and HGO are sent to their respective hydrotreater units in which the pseudo-components heteroatoms are removed via catalytic treating. However, the vacuum residue is sent to a Canmet slurry hydrocracker so as to be upgraded into an oil fraction with a lower average boiling point. Subsequently, the hydrocracker lighter products are separated and hydrotreated whereas the hydrocracker residue is withdrawn and gasified.

The gasification section is where steam, power and hydrogen are produced. Instead of being recycled to the hydrocracker for a higher overall conversion, the viscous and dense hydrocracker residue is gasified in an entrained up-flow slagging gasifier that eventually produces hydrogen and carbon dioxide. The CO_2 is captured and sequestrated via amine absorption whilst the hydrogen is partly recycled to the upgrading facility's hydrocracker and hydrotreater units and partly fed to a high hydrogen combined cycle for steam and power production. Thus, the produced hydrogen flow rate has to be sufficiently high to satisfy the demand of the upgrading units and produce significant amount of power and steam to maintain the utility self-sufficiency of the IGCC process.

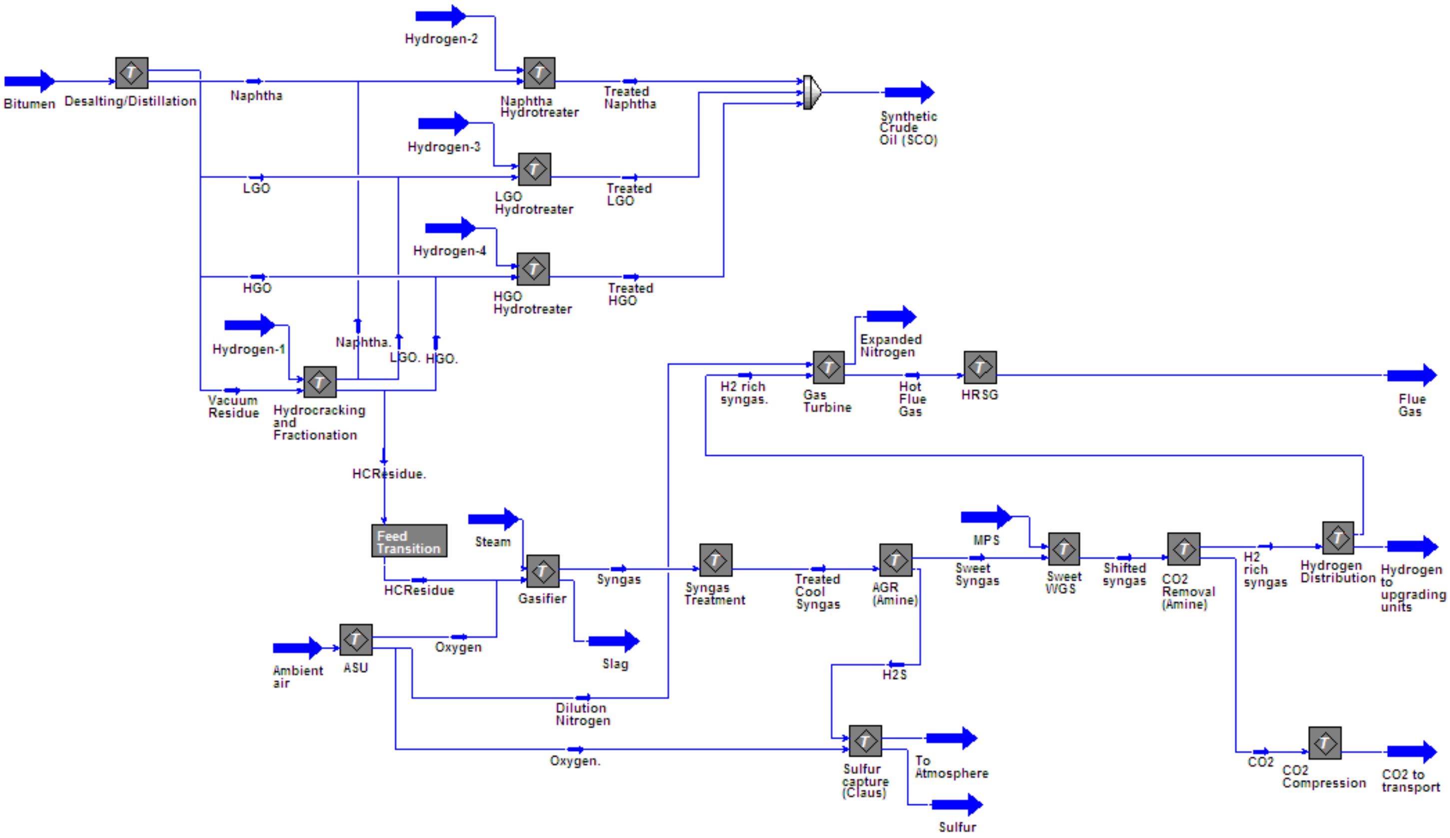

Figure 2.3: Simplified flowsheet of the integrated bitumen upgrading and gasification process

2.5. <u>Petroleum upgrading process</u>

2.5.1. Atmospheric and vacuum distillation

The desalter and atmospheric and vacuum distillation sections description and their simulation are detailed in chapter 3.3.1.

2.5.2. Hydrocracking

Hydrocracking is a reaction that consists of breaking larger hydrocarbon molecules to produce a lower boiling point and lower density petroleum product fraction. The reaction consists of thermal and catalytic mechanisms. Thermal cracking occurs when molecules naturally split due to the highly exited state of the system, at temperatures exceeding 350ºC, and can be promoted by acid sites provided by a catalyst, e.g. alumina and zeolite, present in the system. Catalytic cracking on the other hand requires the addition of a metal to the catalyst active site and a high hydrogen pressure in order to promote hydrogenation which saturates the free radicals produced from the thermal split. Effectively, hydrocracking can consist of the scission of large paraffin molecules, the hydrogenation of free radicals, the dealkylation of an attached alkyl group and the hydrodecyclization of a cyclic compound.

The hydrocracking of bitumen and heavy oils is usually referred to as hydroconversion or hydroprocessing. A hydroconversion reactors' main function is hydrocracking where some hydrotreating inevitably occurs because of the abundance of heteroatoms in the heavier oils feeds. The trickle-bed, ebulated-bed and slurry reactors are three types of three phase hydroconversion units operated in the petroleum industry (see Figure 2.4). The hydrogen, acid gas and the lighter petroleum components are present in the gas phase, the liquid phase contains mainly the heavy petroleum feed undergoing upgrading while the solid phase constitutes mainly of the reactor catalyst.

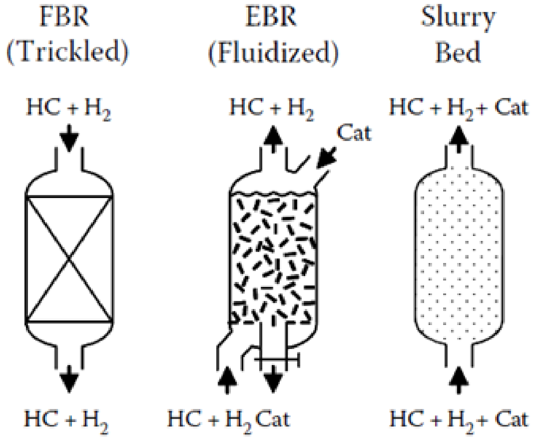

	FBR	EBR	Slurry
Pressure, MPa	100-200	100-200	100-300
Temperature, °C	380-420	400-440	420-480
Unit LHSV, h^{-1}	0.1-0.5	0.2-1.0	0.2-1.0
Max. Conv. to 550°C-, wt%	50-70	70-80	80-95
Unit cycle length, months	6-12	Cont. opn.	Cont. opn.

Figure 2.4: Different types of reactors used in the hydroconversion of heavy petroleum feeds [4]

<u>Slurry Phase Reactors</u>

The slurry phase hydroprocessing technology is a not common in the current commercial petroleum upgrading industry. In a slurry phase processes, a fine catalyst or additive powder (usually from 0.1 to 5wt%) is mixed with the petroleum heavy feed and charged into a reactor vessel where it flows upwards with hydrogen gas bubbling through the solid/liquid mixture and turbulently mixing the three-phase flow. Consequently, a uniform temperature distribution is observed in slurry hydrocracker reactors. A recycle flow is present for the gas and slurry phase separated at the outlet of the reactor in order to lower operating costs. The recycled hydrogen reduces the hydrogen demand of the unit while the slurry phase recycle increases overall conversion and reduces the catalyst utilization [4].

The slurry process is an attractive technology because of its high residue conversion, regardless of the heteroatom content and "dirtiness" of the feed. The added powder increases the hydrogenation activity in the reactor and mitigates coke formation by inhabiting the mesophase in its porous structure and hindering the large carbon cores to amalgamate [58]. More than 10 slurry hydrocracking technologies have been researched worldwide on a pilot scale with some already industrialized. Some processes are the VEBA-COMBI-Cracking (VCC) which is a German process adopting a red mud iron additive, the Exxon-Mobil M-Coke technology developed with a molybdenum naphthenate catalyst, the Venezuelan HDH technology which utilizes a local inexpensive iron ore and the Canmet slurry hydrocracking technology which operates with an iron sulfate catalyst [3, 59, 60]. The main downside of the slurry hydrocracking process falls in the extremely high catalyst utilization. Since the fine powder is mixed with the feed, it exits the reactor in the pitch and is difficult to economically separate and regenerate [6, 61].

Catalyst choice

The chosen catalyst for the integration of the hydrocracking and gasification technologies is an iron based catalyst. Although iron has a low hydrogenation activity, it is the metal of choice in many worldwide slurry hydrocracking processes [60]. To compensate for its lower activity, operating temperatures and hydrogen pressures are usually increased to boost thermal cracking and reduce coking, respectively. The presence of iron in the slurry hydrocracker is beneficial for the reasons that follow [6, 62].

Slag viscosity reduction

Gasification is a reaction in which a carbon-based feedstock reacts with limited amounts of oxygen in order to produce CO and hydrogen. The slagging-type gasifier is the technology chosen for this upgrading process which are high energy consuming reactors since they usually operate at temperatures that exceed 1300ºC in order to avoid reactor fouling caused by molten ash clogging. Iron addition to the gasification unit is found to be beneficial since it has the potential to decreases the viscosity and melting point of the slag [27, 28]. Less viscous slag allows for the reduction of the reactor operating temperature since the molten ash can exit the reactor at much faster rate while melting at lower temperatures. The metal addition therefore reduces energy consumption, making the process more sustainable, economical and environmentally friendly.

Coke inhibition

Coking is a reaction that has to be avoided during hydrocracking reaction. Coke can deposit at the bottom of equipment causing the units to foul and scale [63]. The addition of iron is a cheap alternative to hinder the coking reaction and allow the operation of the hydrocracker at a higher temperature. The reaction rate of both coking and cracking reactions increases with temperature therefore it is important to introduce a metal into the hydrocracker in order to hamper undesired reactions.

In order to hinder coking, the iron is transformed into iron oxide at a temperature of 474ºC. After coming into contact with H_2S, the iron is sulfided. The iron sulfide, a black granulated insoluble solid, promotes the adhesion of the mesophase (coke precursor) to its surface. By holding on to the mesophase, the iron sulfate impedes its agglomeration, reducing the total coke formation inside the reactor [11]. Moreover, fine catalyst addition reduces the mass transfer limitations associated with catalyst particles of larger sizes. Therefore, regardless of the activity of the catalyst, the rapid free-radical stabilization with hydrogen addition due to the rapid kinetics associated with the micron-scale added catalyst allows for higher operating temperatures without an increase in coke formation.

Catalyst price and utilization

One of the main advantages of using iron is in the cost of the transition metal. Iron is the cheapest of all the transition metals shown in Table 2.2. Compared to molybdenum, iron is around 1000 times cheaper. Iron is more frequently used in slurry hydrocracking due to its high consumption. Up to 5wt% catalyst can be added to the petroleum feedstock therefore iron is chosen instead of the other metals since it can still provide some catalytic value to the reaction without dramatically increasing the reactor operating costs. Some developed hydrocrackers did utilize molybdenum as a catalyst (like the M-Coke hydrocracker of ExxonMobil) but they remained on pilot scale due to their high running cost [60].

Table 2.2: Average prices of metals on March 29, 2012

Metal	Price ($/kg)
Iron	0.08
Nickel	27.13
Cobalt	73.70
Molybdenum	73.85
Ruthenium	17,682.91
Gold	54,167.58
Platinum	53,286.65

Slurry hydrocracking kinetics

Numerous kinetic studies have been performed for the hydrocracking reaction of individual hydrocarbon molecules. Kinetic models were developed for the hydrocracking of n-heptane [64, 65], n-octane [66, 67] and n-decane [68, 69] over a variety of catalysts. Langmuir-Hinshelwood kinetic models [70] were applied for the hydrocracking of simple hydrocarbon molecules, describing chemisorption onto the active the catalyst surface. On the other hand, the hydrocracking of a heavy feedstock is an array of complex reactions with plenty of molecules.

When dealing with heavy petroleum feeds, physical properties such as density and viscosity can vary significantly depending on the present fraction such as light ends, middle distillates and asphaltenes. The obtained kinetics also depends on scale of operation. Microautoclaves used for hydrocracking are limited since only a small sample of catalyst and feed are allowed in the system. The most adequate economical scale for the study of the hydrocracker kinetics is the bench scale reactor where the reacting environment can be downscaled adequately [6].

Canmet slurry hydrocracker model

In 1930, Canmet developed a hydrocracking unit on a laboratory scale with a 10L reactor vessel for hydroconversion of heavy fuels. The Canmet hydrocracker has evolved quite significantly since and has recently been deemed as the most efficient approach to a commercially viable slurry hydrocracking technology by Universal Oil Products (UOP). In 2006, UOP began working with NRCan in order to evaluate and advance the Canmet hydrocracking process. After a couple of pilot plant tests, UOP obtained worldwide rights to license the Canmet hydrocracker [60, 71].

The hydroconversion reactor model developed by UOP is confidential and proprietary. Since the overall hydrocracking and gasification integration process proposed contains a Canmet hydrocracker, it is necessary to propose a reactor of model that characterizes the unit in order to represent its behavior in the upgrading simulation. Being unable to divulge the UOP licensed hydrocracker data, Canmet was able to provide a couple of test runs from 1979 that took place in the 5,000 BPD pilot facility built for Petro-Canada's Montreal facility [63, 72-75].

Multiple runs were performed in the Petro-Canada facility with hydroconversion temperatures ranging from 400ºC to 480ºC for an Athabasca bitumen feed where the residue conversion was recorded. Unfortunately, hydrotreating and hydrocracking selectivity were not extensively documented for the hydroconversion of the Athabasca bitumen in the slurry reactor, therefore only the residue conversion kinetics were accurately modeled using the Canmet data. The product distribution based on boiling point and the heteroatom removal characteristics were annexed to the Canmet model using more recent hydroconversion experiments in an H-Oil ebullated-bed reactor [69, 76]. The reactor model is explained in section 3.3.5.

2.5.3. Hydrotreaters

The naphtha, light gas oil and heavy gas oil hydrotreaters description and their model implementation are detailed in chapter 3.4.

2.6. Gasification process for hydrogen production

The gasification process is described in details in chapter 4.2 which also presents the benefits of its integration with the upgrading facility.

2.6.1. Air Separation Unit

The air separation unit description and its simulation are detailed in chapter 4.2.1.

2.6.2. Gasification

The process of gasification consists of converting solid carbon feeds in various forms reacting with oxygen and/or steam into carbon monoxide, carbon dioxide, hydrogen, steam and methane [49-51, 77]. The gasification reactions are shown below in equations 2.3 to 2.10:

Combustion reactions

$$\mathrm{C} + \frac{1}{2}\,\mathrm{O_2} \rightarrow \mathrm{CO} \tag{2.3}$$

$$\mathrm{CO} + \frac{1}{2}\mathrm{O_2} \rightarrow \mathrm{O_2} \tag{2.4}$$

$$\mathrm{H_2} + \frac{1}{2}\mathrm{O_2} \rightarrow \mathrm{H_2O} \tag{2.5}$$

Boudouard reaction

$$\mathrm{C} + \mathrm{CO_2} \rightleftarrows 2\,\mathrm{CO} \tag{2.6}$$

Water-gas reaction

$$\mathrm{C} + \mathrm{H_2O} \rightleftarrows \mathrm{CO} + \mathrm{H_2} \tag{2.7}$$

Methanation reaction

$$\mathrm{C} + 2\,\mathrm{H_2} \rightleftarrows \mathrm{CH_4} \tag{2.8}$$

Water-gas shift reaction

$$\mathrm{CO} + \mathrm{H_2O} \rightleftarrows \mathrm{CO_2} + \mathrm{H_2} \tag{2.9}$$

Methane steam reforming reaction

$$\mathrm{CH_4 + H_2O \rightleftarrows CO_2 + 3\ H_2} \tag{2.10}$$

Some important parameters in gasification thermodynamics are the oxygen and water to carbon ratio and the heat loss in the system. It is necessary to control the gasifier's operating condition in order to control the product concentration. The methane content should be kept at a minimum which is why the gasifier is operated at temperatures above 1300ºC but exceedingly high temperatures can also damage the vessel and equipment of many types of gasifiers, while reducing the process efficiency due to extensive heat loss. For a more detailed thermodynamics and reaction kinetic description, refer to chapters 2 and 3 of C. Higman and M. van der Burgt's book [50].

More details on the gasifier and its simulation are provided in chapter 4.2.2.

2.7. __Acid Gas Removal__

The COS hydrolysis removes sulfur traces in order to avoid downstream catalyst poisoning issues [78].

$$\mathrm{COS + H_2O \rightleftarrows CO_2 + H_2S} \tag{2.11}$$

The COS hydrolysis is a slightly exothermic equimolar reaction (see equation 2.11) that is promoted by an activated alumina catalyst, e.g. Hydrocel 630 or Hydrocel 640 [79]. The reaction is recommended to take place at temperatures between 177ºC and 204ºC with a residence time high enough to convert over 99.5% of the COS into H_2S, for optimal acid gas removal [80]. Due to the low concentration of COS in the syngas, the reactor operation is effectively isothermal.

The next step in the syngas treatment process is H_2S and CO_2 removal. Essentially, the concentration of CO_2 in the syngas is insignificant if compared with the WGS or the GT product stream which makes it trivial compared to the H_2S concentration in the AGR step that precede the sweet WGS. CO_2 and H_2S can be removed with different technologies like physical or chemical solvent absorption, solid absorption and membrane permeation [81]. Guidelines for selecting the AGR process are presented in Table 2.3. Since the IGCC process is a large operation that generally operates at high pressure with considerable amounts of sulfur, it is recommended to utilize an alkaline solution or physical absorption for the AGR process.

Table 2.3: Guideline for the selection of an H_2S and CO_2 removal process [81]

Type of process	**Acid gas**		**Plant size**	**Partial pressure**	**Sulfur capacity**
	H_2S	**CO_2**			
Absorption in an alkaline solution	Applicable	Applicable	High	Low	High
Physical absorption	Applicable	Applicable	High	High	High
Membrane permeation	Applicable	Applicable	Low	High	Low
Adsorption	Applicable	Applicable	Low	Low	Low

The conventional absorption technique consists of counter-currently contacting a lean solvent with the acid gas in an absorption column which sweetens the product by enriching the solvent with CO_2 and H_2S (see Figure 2.5). The rich solution is regenerated in a thermal regeneration unit where the acid gas is released from the solvent that can afterwards be cooled and recycled to the absorber.

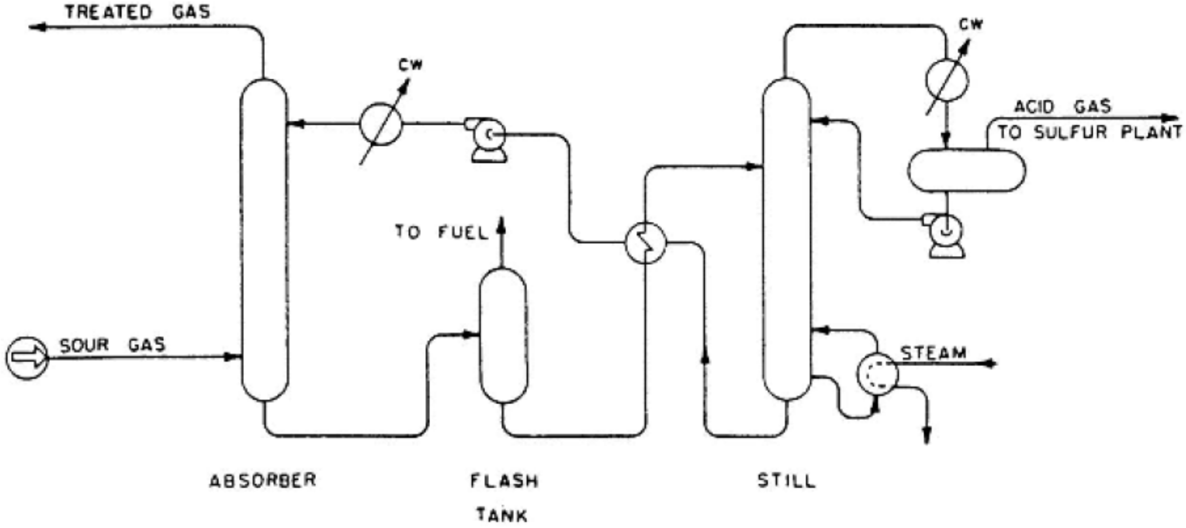

Figure 2.5: Typical amine treatment simplified process [7]

AGR via alkaline solution consists of adsorption with chemical solvents which is less dependent on partial pressure. Solvents like ethanolamine (MEA), diethanolamine (DEA) or methyldiethanolamine (MDEA) react exothermally with the CO_2 and H_2S at temperatures around 40ºC, forming a weak chemical bond that can be thermally broken in the solvent regeneration unit operating at near boiling point temperature. Physical adsorption on the other hand involves the absorption of the acid gas into organic solvents that have a high solubility for CO_2 and/or H_2S. The operation of physical process, e.g. the Rectisol, Sulfinol or Selexol process, generally requires lower operating temperatures and higher pressures than chemical solvents in order to increase acid gas solubility. The regeneration of the physical solvent also occurs at high temperatures and low pressure at which point gas solubility diminishes significantly.

The CO_2 separation process first started in the 1970s for enhanced oil recovery and not for reduction of greenhouse effects [82]. The mostly used chemical absorbent and the one utilized in this process is a monoethanolamine (MEA) based solvent. MEA was developed over 70 years ago as a non-selective absorption solvent for CO_2 and H_2S removal and is the most widely used type of solvent for the removal of acid gases from natural gas streams [83]. The synthetic gas produced by the gasifier contains high quantities of sulfur with relatively low CO_2 concentrations which does not necessitate a selective H_2S separation.

MEA is usually limited to 10-30 wt% in solution so as to avoid corrosion problems with a loading 0.3-0.35 moles of acid gas per mole of amine for carbon steel and loadings as high as 0.9 moles of acid gas per mole of amine for stainless steel equipment [84]. H_2S and CO_2 are non-selectively and reversibly removed with this amine solvent while COS and CS_2 irreversibly react with the solvent which result in solution loss in the system which validates the use of a COS hydrolysis reactor prior to amine treatment [83]. MEA is an amine with a relatively high biodegradability compared to other amines like 2-Amino-2-methylpropanol (AMP) or methyldiethanolamine (MDEA) which means that it has almost no adverse effect on the well being of the flora and fauna, however large quantities can of MEA emissions can cause eutrophication or acidification after decomposition [85].

The simulation of the AGR in Aspen HYSYS® is explained in chapter 4.2.3.

2.8. Water Gas Shift

The water gas shift process description and its simulation are detailed in chapter 4.2.4.

2.9. Power generation units

The combustion turbine unit and the heat recovery steam generation process and their simulation are detailed in chapter 6.

2.10. CO_2 compression

The carbon capture occurring in the AGR section requires compression and pumping in order to effectively transport and sequestrate the separated CO_2. Corrosion and hydrate formation are the main concerns during this process. Therefore, the CO_2 stream should meet the design specifications shown in Table 2.4 [80].

The carbon separated from the syngas before its combustion in the GT is compressed and cooled for a more efficient transportation. The CO_2 phase diagram presented in Figure 2.6 depicts the phase behaviour of CO_2 in function of temperature and pressure in which two important points are shown. The triple point at 56.6ºC and 0.511 MPa is where the solid, liquid and gas states can co-exist. Below the aforementioned temperature and pressure, CO_2 can only be present in the gas and solid states. The second important point in Figure 2.6 is the critical point at 31.4ºC and 7.38 MPa. Above this critical pressure and at moderate temperatures, the CO_2 is in a dense supercritical phase and behaves like a liquid. With a density of 800-1200 kg/m^3 which is similar to water, carbon dioxide can transported more efficiently if it is in the supercritical state [83, 86].

Table 2.4: Pipeline specifications for CO_2 sequestration [80]

Parameter	Units	Parameter Value
Inlet Pressure	MPa (psia)	15.3 (2,215)
Outlet Pressure	MPa (psia)	10.4 (1,515)
Inlet Temperature	°C (°F)	35 (95)
N_2 Concentration	ppmv	< 300
O_2 Concentration	ppmv	< 40
Ar Concentration	ppmv	< 10
H_2O Concentration	ppmv	< 150

The CO_2 compressor train is simulated in Aspen HYSYS® with inter-stage coolers that take care of cooling down the compressed steam while condensing the residual moisture from the AGR section. Glycol dryers can also be located at the mid-point of the compressor trains if the CO_2 stream water content does not meet the pipeline specifications presented in Table 2.4. The power consumption is determined for the CO_2 power consumption section that should attain a final pressure exceeding 15 MPa and 37ºC [80, 87].

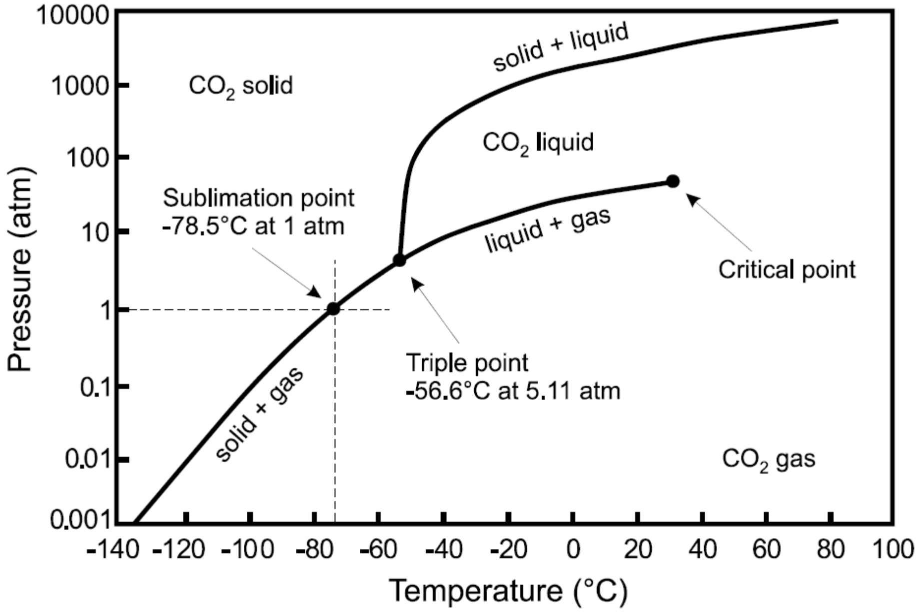

Figure 2.6: CO2 three-phase diagram

2.11. Sulfur recovery – Claus process

The Claus process for sulfur recovery used the current industry is a modification of a process that was first utilized in 1883 in which hydrogen sulfide and oxygen would react in the presence of catalyst in order to form elemental sulfur and water as shown in equation 2.12 [83].

$$H_2S + {}^1/_2O_2 \rightarrow S + H_2O \qquad 2.12$$

Due to the highly exothermic nature of the overall reaction, it was very difficult to control the reacting system therefore the process was divided into two sections. Firstly, the combustion reaction is controlled in a burner section during which half of the H_2S (see equation 2.13) and all of the carried hydrocarbons and combustibles react with a controlled quantity of oxygen. Following the burner is a sequence of reactors dealing with the moderately exothermic catalytic reaction of converting H_2S to sulfur as shown in equation 2.14. However, the reaction is a little bit abstruse because of the various species of gaseous sulfur ranging from S_1 to S_8. Side reactions can also produce COS, CO, H_2 and COS if hydrocarbons are still present in the stream however the combustion conversion was assumed at 100% for all compounds other than sulfur [24, 83, 88, 89]. The combination of equation 2.13 and 2.14 is shown in equation 2.15 and illustrates that hydrogen sulfide reacts with oxygen to ultimately produce elemental sulfur and water.

Combustion reaction

$$H_2S + {}^3/_2O_2 \rightarrow SO_2 + H_2O \qquad 2.13$$

Claus reaction

$$2\ H_2S + SO_2 \rightarrow \frac{3}{x}S_x + 2\ H_2O \qquad 2.14$$

Overall reaction

$$3\ H_2S + {}^3/_2O_2 \rightarrow \frac{3}{x}S_x + 3\ H_2O \qquad 2.15$$

The Claus plant therefore consists of a burner and condenser followed by a series reactors and condensers where sulfur is ultimately produced. The Claus plant configuration depends greatly on the H_2S feed concentration. The GPSA data book proposes different configuration based on the feed sulfur concentration that are presented in Table 2.5 and Figure 2.7 [83].

Table 2.5: Various Claus plant configurations based on the feed stream H_2S concentration [83]

Feed H_2S conc. (mol%)	Claus Process Suggested
55 – 100	Straight-through
30 – 55	Straight-through straight through with acid gas and/or air preheat
15 – 30	Split-flow or straight-through with feed and/or air preheat
10 – 15	Split-flow with acid gas and/or air preheat
5 – 10	Split-flow with fuel added or with acid gas and air preheat, or direct oxidation or sulfur recycle
< 5	Sulfur recycle or variations of direct oxidation or other sulfur recovery processes.

The straight-through Claus process is best suited for the sulfur recovery of the proposed gasification process and is illustrated in Figure 2.8. The sulfur burner temperature ranges between 1093ºC to 1427ºC and is attained by oxidizing of a third of the sufficiently high H_2S concentration. As it was also previously mentioned, hydrocarbons, mercaptans, cyanides, ammonia and other combustibles are also oxidized in the burner at sufficiently high temperatures, in order to avoid corrosion and fouling. The flame temperature should therefore exceed 980ºC and is contingent on the concentration of H_2S in the process feed, which is why various configurations are proposed for Claus processes with low sulfur content. The sulfur capture conversion of the burner is also assumed to never exceed 75 percent before catalytic conversion [80].

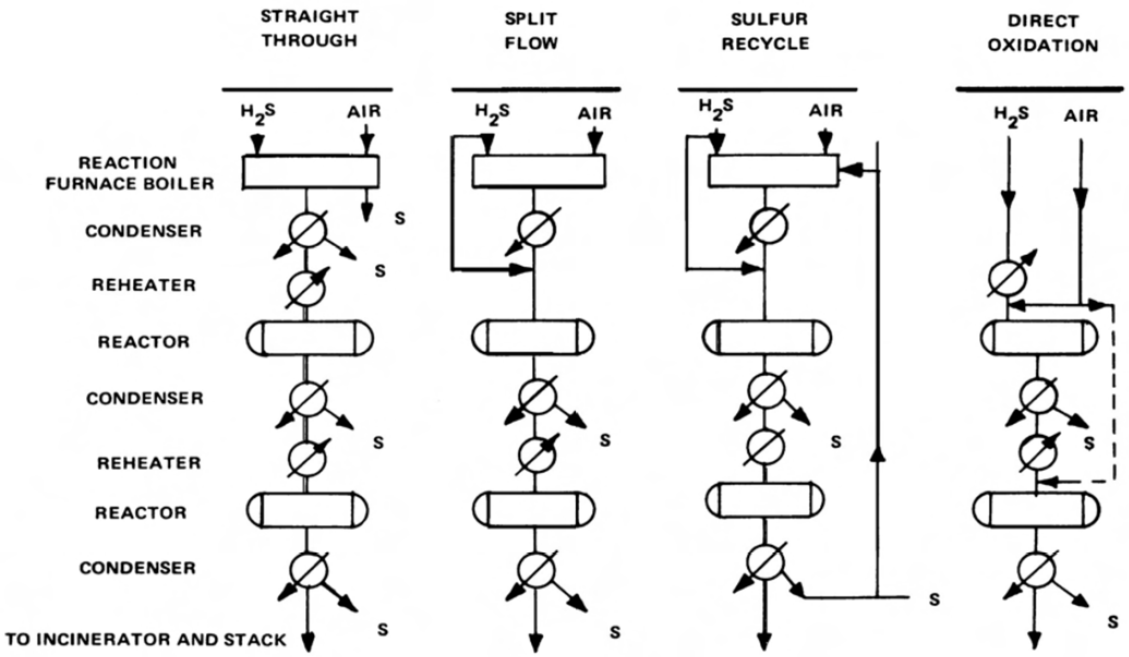

Figure 2.7: Various Claus process configurations [83]

Following the burner are three converter reactors packed with activated alumina catalyst. They respectively operate at temperature of 232ºC, 199ºC and 188ºC in order to achieve a sulfur conversion efficiency exceeding 99% [81, 83]. Since the Claus reaction presented in equation 2.14 is exothermic, lower temperatures are required to achieve higher conversions. However, the hydrolysis of COS and CS_2 attains a higher conversion at higher temperatures which is why the first reactor operates at hotter conditions. The second and third reactors are operated at temperatures that give reasonable reaction kinetic rates and equilibrium conversions while avoiding the deactivation of catalyst associated with molten sulfur viscosity increases that occur at lower temperatures [90].

The burner outlet and inter-stage reactor streams are cooled down by raising HP and LP steam, correspondingly. The HP steam is integrated with the heat recovery steam generation unit while the LP steam is used for process heating purposes. The temperature of the condensers should be between 165-180ºC which yields molten sulfur with reasonably low viscosity [90]. The final condenser temperature is however around 128ºC [81, 83]. The molten sulfur is sent to a sulfur pit where it is handled and stored. More details on "Sulfur storage and handling" are available in the GPSA data book.

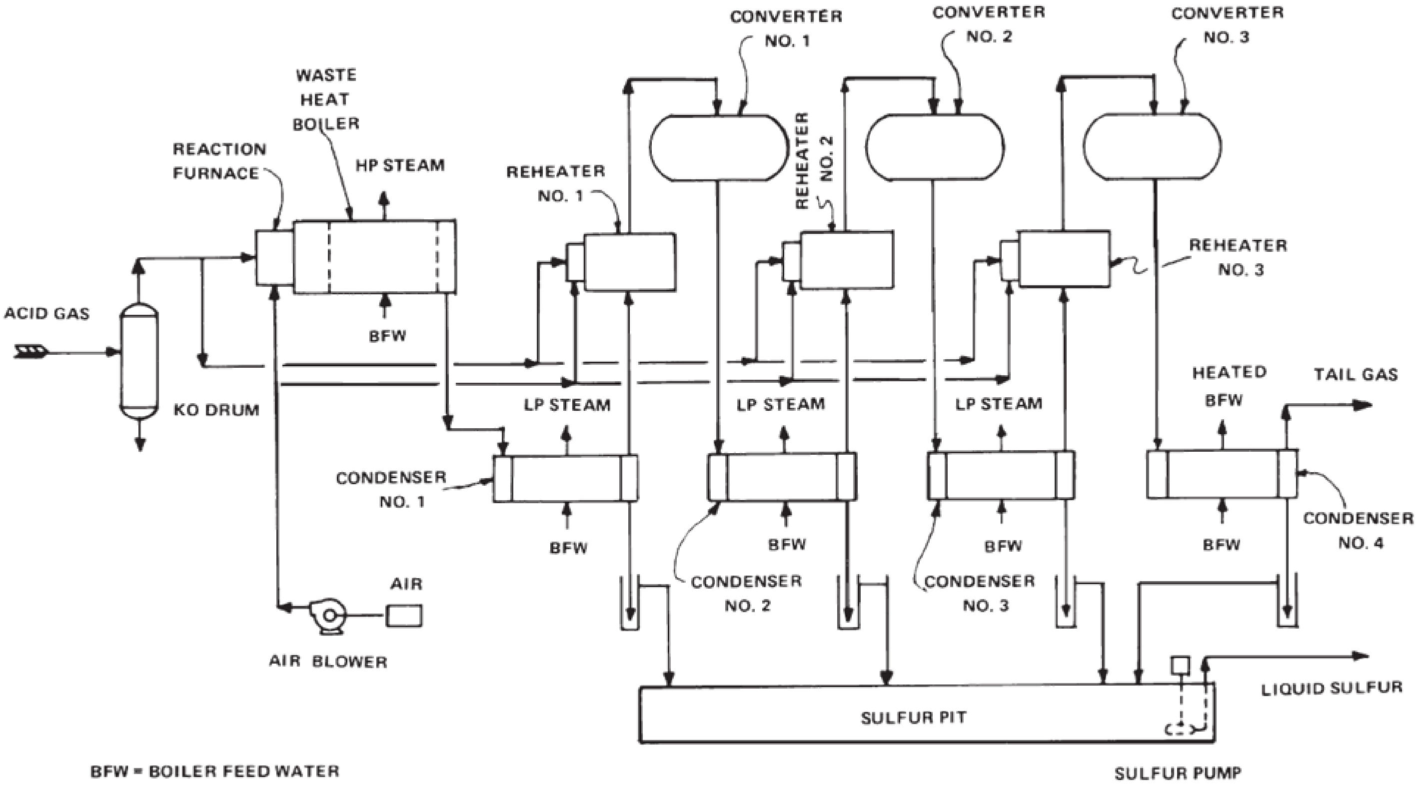

Figure 2.8: Simplified PFD of a straight-through Claus process [83]

3. Simulation of a Bitumen Upgrading Facility Utilizing the Canmet slurry hydrocracker Technology

3.1. Introduction

Petroleum upgrading of heavy oils, such as bitumen, is necessary compared to conventional crudes in order to remove their excessively high sulfur and nitrogen content and reduce of their overall boiling point and density [1, 3, 4]. Dubbed as unconventional oils, the world's bitumen and extra-heavy oils are primarily concentrated in the Canadian province of Alberta and the Orinoco Belt in Venezuela. About 6 trillion barrels have been identified worldwide with an estimated recoverability of 1 to 2 trillion barrels [91].

The world oil demand is predicted to rise from 85 to 105 million barrels per day [1]. Moreover, countries not belonging to the Organization for Economic Co-operation and Development (OECD) are forecasted to represent 93% of the increase in global energy demand between 2007 and 2030. Unconventional oil derived synthetic crudes currently holds a small share of the energy [1]. However, since it consists of about 30% of the world oil reserves, the impact of heavy oils are likely to increase to effectively contribute to the future world oil market, which is contingent on the maturity and progress of petroleum upgrading technologies.

The current upgrading technologies are based on carbon rejection or hydrogen addition. The carbon rejection procedure, which represents 56.6% of the total worldwide processing capacity, consists of reducing the carbon percentage in the oil product via thermal cracking [2, 3]. This leads to the formation of a solid amalgamated carbonaceous by-product called "coke". An increase in coking conversion tends to produce lighter petroleum fractions to the detriment of the mass yield of the product [3-11]. Conversely, hydrogen addition consists of cracking the hydrocarbons in a hydrogen rich environment which effectively reduces the carbon to hydrogen ratio while mitigating coke formation. Hydrocracking, hydrotreating and hydroconversion are well-known hydrogen addition upgrading technologies used in today's petroleum industry [4, 8].

The industrial processes available for upgrading heavy oils are configured based on various characteristics such as feed type and product selectivity and price [2, 4, 10, 92]. In this work, the Canmet slurry hydrocracker was selected and annexed to naphtha (b.p. 40-180ºC), light gas oil (b.p. 180-360ºC) and heavy gas oil (b.p. 360-540ºC) trickle-bed hydrotreaters (see Figure 3.1). The upgrading process seeks to produce a high quality Synthetic Crude Oil (SCO) from Canadian bitumen via high hydrocracking and hydrotreating conversions while withdrawing the hydrocracker residue (540+ºC) and potentially charging it into a gasification process for hydrogen production. The Canmet slurry hydrocracking technology has the potential to reach high conversion while mitigating coke formation via the use of inexpensive fine iron based catalyst (1-5wt%) that is recovered in the hydrocracker residue.

Heavy oil upgrading process configurations that involve the gasification of heavy oil residue are or will be in commercial operation. The Long Lake integrated upgrading project operated by Nexen Inc. is a steam assisted gravity drainage (SAGD) oil operation integrated with an upgrading facility that processes approximately 72,000 BPD. The Long Lake operation uses the OrCrude™ process from which deasphalted bottoms are gasified in four Shell Gasification Process trains in order to ultimately produce the required hydrogen for their hydrocracking operation and syngas fuel that can be utilized for SAGD or cogeneration (Cogen) operations.

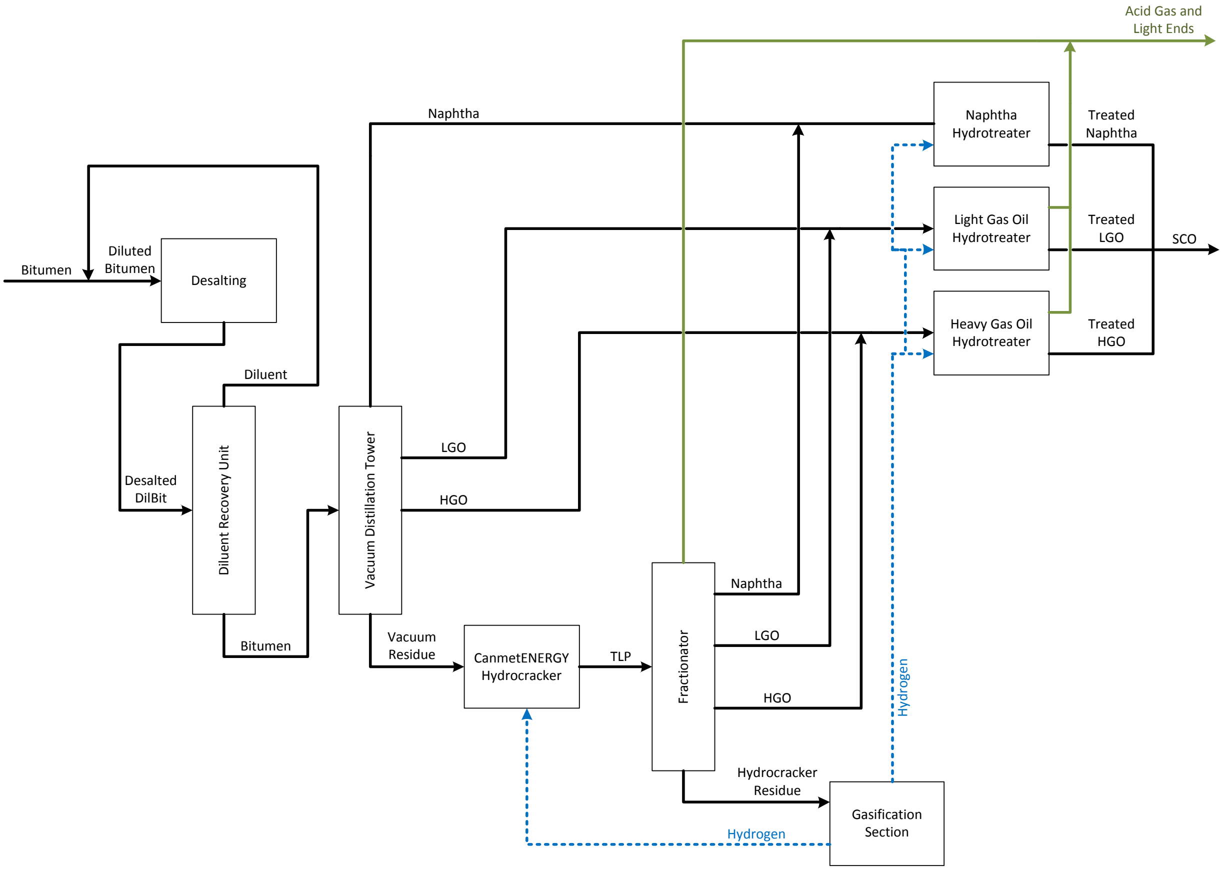

Figure 3.1: Simplified block flow diagram of the proposed bitumen upgrading process

Considering a 100% availability, the Nexen Inc. operation should produce about 59,000 BPD of Premium Sweet Crude [29, 93]. The North West Upgrading Inc. facility is another ongoing project that plans to combine the LC-Fining technology and a heavy petroleum residue gasifier [94]. Finally, the Shell Pernis Refinery in Rotterdam, Netherlands also included a gasification process in their plant in order to produce synthetic gas from heavy visbreaking residue or straight-run vacuum residue [31].

The proposed upgrading process contains three major types of units: distillation towers, the Canmet slurry hydrocracker and the naphtha (NPH), light gas oil (LGO) and heavy gas oil (HGO) hydrotreaters. They are modeled and simulated in Aspen HYSYS® where the bitumen is characterized in the software oil environment. The goal of the simulation is to determine the hydrogen, utility and power consumption of the upgrading process relative to the SCO quality. Moreover, the amount of carbon dioxide emitted during the oil recovery and upgrading processes is estimated based on correlations identified in the literature. The simulation of a bitumen upgrading process, which contains petroleum distillation units, a hydroconversion reactor and hydrotreaters, is rare in the current public literature [56]. The results of such a simulation can be integrated with additional processes, e.g. integrated gasification combined cycle, in order to evaluate the feasibility and optimize the operation of such potential ventures.

3.2. Simulation tools

3.2.1. Simulation software

Aspen HYSYS® is as a market-leading process modeling tool frequently used in the petroleum upgrading and refining industry by companies like Petrobras, Preem and PTT [43]. The program contains a user friendly graphical user interface (GUI) that is ideal for building, customizing and combining large simulations. Aspen HYSYS® also authorizes user variables, model customizations and software extensions to VBA, aspenOne, and Microsoft Excel. [44, 45] The software is equipped with a strong thermodynamic foundation and a variety of property packages [46, 47]. Containing over 1,000 pure components, Aspen HYSYS® also has the option to create hypothetical compounds and assist the user in defining crude oil assays in its Oil Environment in which fluid properties and characteristics can be specified or estimated with several embedded correlations.

3.2.2. Feed characterization

The Aspen HYSYS$^{®}$ characterization of crude oil is executed in the simulator Oil Environment where a petroleum assay is primarily defined by its boiling point distribution, density, molecular weight, viscosity, and light end composition. The entered data helps generate hypothetical pseudo-components that characterize the defined crude assay. The software generates and displays a simulated distillation curve allowing the user to visually verify the characterized petroleum fraction. Oil properties are estimated with various embedded correlations if they are not available experimentally. However, it is advised to thoroughly characterize the feed with experimental data in order to better define the system [44]. The additional Aspen HYSYS$^{®}$ Refining license permits the user to individually vary the property of each pseudo-component, allowing characteristics like the heteroatom content, the aromatic content, the density, the molecular weight, the viscosity and the C to H ratio to be changed for individual components [48].

3.3. Process description

The proposed heavy oil upgrading plant, presented in Figure 3.1, is simulated with a feed of 100,000 BPD of Athabasca bitumen (see Table 3.1) that undergoes atmospheric and vacuum distillations in order to separate the original petroleum mixture into light ends, NPH, LGO, HGO and vacuum residue (VR). The NPH, LGO and HGO are sent to their respective hydrotreater units in which the pseudo-components heteroatoms are catalytically removed. However, the VR is charged into a Canmet slurry hydrocracker for upgrading. Subsequently, the hydrocracker's lighter products are fractionated and hydrotreated whereas the hydrocracker residue is withdrawn and has the potential to be gasified for hydrogen production.

Table 3.1: Athabasca bitumen feed properties [56]

API gravity	10.57ºAPI
Sulfur content	4.304 wt%
Nitrogen content	5,423 ppmwt
ASTM D86 5%	196.5ºC
ASTM D86 95%	725.4ºC
C to H atomic ratio	1.53

3.3.1. Atmospheric and vacuum distillation

Bitumen is a dense and viscous petroleum substance that does not flows easily at ambient conditions [95]. For transportation purposes and to avoid precipitation, the Athabasca bitumen feed is blended with NPH, forming diluted bitumen (dilbit) [10, 96]. The volumetric ratio of bitumen to NPH is adjusted in order to obtain a dilbit with a density of 17ºAPI [97]. Afterward, the blend is pumped and heated before going through desalting. The simulation utilizes the Peng-Robinson thermodynamic package which can accurately characterize hydrocarbon interactions and is the most suitable model in Aspen HYSYS® as it has the largest temperature and pressure applicability range with the largest binary interaction parameter database [44, 46, 98].

3.3.2. Desalting

Petroleum crude oil contains dissolved and suspended crystalline salt particles present mainly in the emulsified water fraction. The desalting process therefore consists of a water washing procedure that removes the crude salt fraction when it exceeds 10 lb salt/1000 bbl oil [7]. Heavy oils are usually rich in NaCl and solid particulates which is why they are often water washed in order to avoid solid depositions which can lead to fouling and corrosion of process units. The water utilization is dependent on the flow rate, density, viscosity and pH of crude (see Table 3.2). The desalting of Athabasca bitumen is simulated at a temperature of 150ºC with a water injection of 10 vol% of the bitumen feed. For optimal dehydration, the pH value should be maintained between 6 and 8 [5, 7, 99]. Therefore, 86 m^3/h of water is injected into a two stage desalting system in order to wash the diluted bitumen with 19 kg/h of demulsifier.

Table 3.2: Heuristics regarding the desalting operation relative to the density, viscosity and volumetric flow rate of oil [7]

Temperature (ºC)	Water wash (vol%)	Gravity (ºAPI)
115 – 125	3 – 4	> 40
125 – 140	4 – 7	30 – 40
140 – 165	7 – 10	< 30

3.3.3. Diluent Recovery Unit

For flow enhancement purposes, the Athabasca bitumen viscosity was reduced by blending with NPH. However, the bitumen rheology's temperature dependency causes the viscosity to decrease significantly at temperatures above 100ºC [100]. Consequently, the diluent has to be separated from the bitumen in an atmospheric diluent recovery unit (DRU) in order to reduce the size of subsequent operating units (see Figure 3.2). The dynamics of the DRU are simplified by flashing the light ends from the dilbit prior to distillation. The DRU is simulated as a 32 tray column as atmospheric fractionators are usually between 30 and 50 trays [7, 99]. The tower operates at a bottom tray temperature of 186ºC, yielding a NPH overhead stream with a TBP at 95% of 180ºC. Stripping steam is injected at the bottom section of the tower in order to remove the sour gas and remaining lighter hydrocarbons while reducing the crude's partial pressure and the required vaporization temperature [7]. The separated NPH is partially recycled as a bitumen diluent while the residual quantity is sent to the NPH hydrotreating unit. The DRU liquid bottom stream consists of a heavy petroleum fraction with a density of 9.77ºAPI which is nearly equal to that of the bitumen.

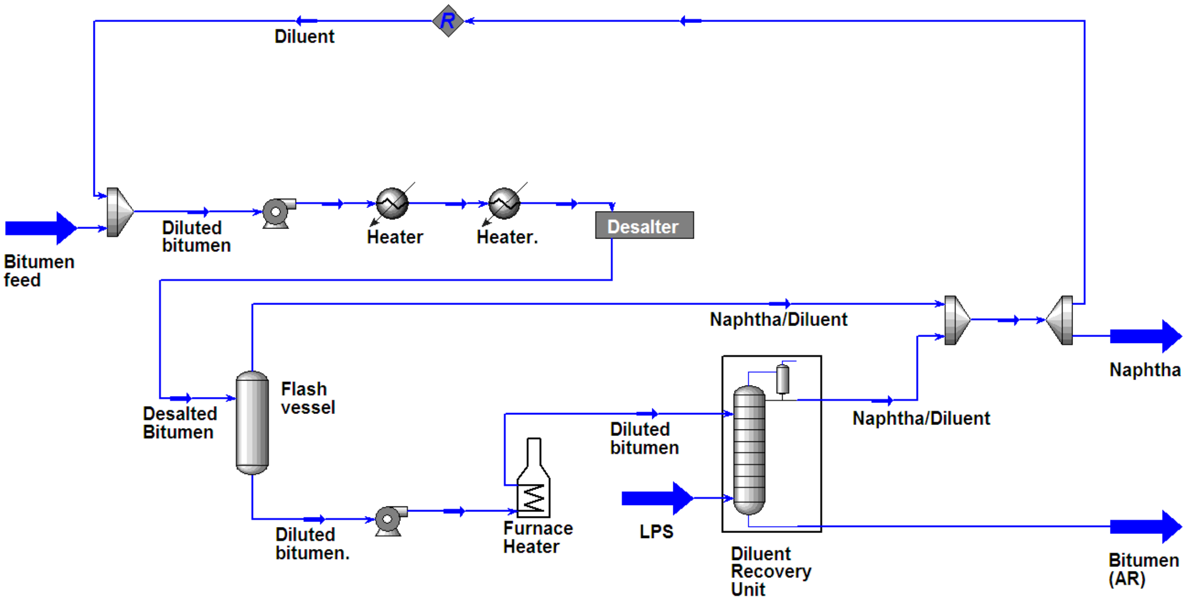

Figure 3.2: Simplified flowsheet of the atmospheric distillation simulation

3.3.4. Vacuum distillation

The DRU bottom product is preheated to a temperature of 360ºC before entering a 24 tray vacuum distillation tower [99]. Increasing the operating temperature above 400ºC is ill-advised since carbonaceous deposits caused by thermal cracking start to form and hinder the tower operation. A superheated stripping steam is also introduced at the bottom of the tower to control cracking by reducing the hydrocarbon residence time in the tower while stripping residual light oil and sour gas. The simulated vacuum distillation tower operates at a condenser pressure of 2 kPa and bottom tray pressure of 5 kPa. Light ends and NPH are the lightest vacuum distillation products and consist of residual light crude from the DRU with a boiling point below 180ºC. The NPH overhead stream and the LGO and HGO side draws are directed to the relevant hydrotreating unit while the 540+ºC vacuum residue bottoms are directed to the hydrocracker (see Figure 3.3).

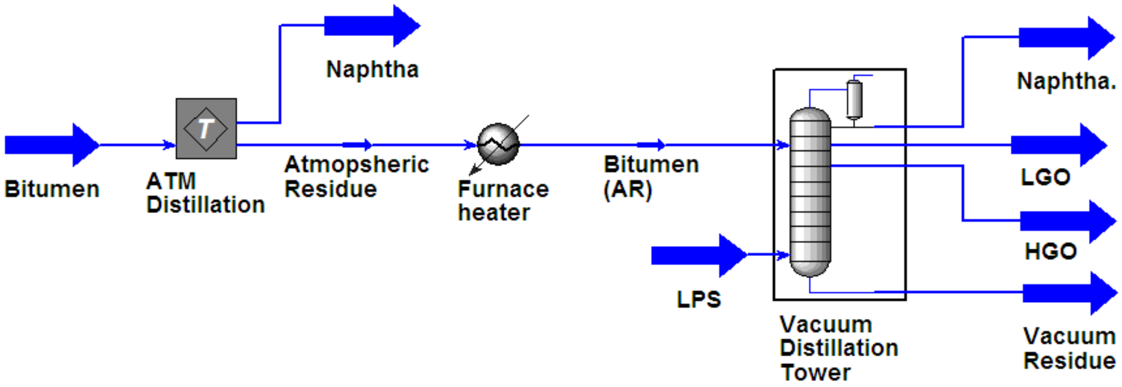

Figure 3.3: Simplified flowsheet of the vacuum distillation tower simulation

3.3.5. *Hydrocracking*

The Canmet slurry hydrocracker operates with an inexpensive coke-inhibiting bifunctional catalyst, which consists of a porous acidic support that promotes thermal cracking whilst dispersed metal oxides and sulfides facilitate C-C bond cleavage via the hydrogenation reaction [3, 101]. The catalyst is prepared from iron sulfate [$Fe_2(SO_4)_3$] and permits the use of high operating temperatures which result in high residue conversions and low coke yields [42, 75]. In comparison to other metals, iron is the least active hydrogenation catalyst [62] but its low cost, high rate of utilization and potentially positive effect on slag rheology for downstream gasification make it an attractive hydrocracking additive.

Universal Oil Products purchased the worldwide rights and license of the Canmet slurry hydrocracking process in 2006. Since then, data generated by the company have been proprietary and thus the simulated Canmet slurry hydrocracker model had to be developed for this study with data obtained from experiments performed primarily during the 1970s when research was active at Canmet [63, 72-75]. These tests consisted of hydrocracking Athabasca bitumen in a slurry hydrocracker of 4.25 litres operated at temperatures of 420-470ºC and pressures of 10-17.89 MPa.

3.3.5.1.Reactor model

The slurry hydrocracker model is sectioned in two parts. Due to the limited amount of Canmet data regarding product mass yield distributions and heteroatom removal, the first section of the model estimates the residue conversion based on operating parameters such as temperature, hydrogen partial pressure and liquid hourly space velocity (LHSV). The proposed reaction shown in equation 3.1 is assumed to be a first order liquid phase forward reaction. The system operates on a mass basis because a mole characterization is difficult when dealing with a variety of large carbon-based molecules such as residues and coke. Similar simplified models were proposed previously for various upgrading units due to the complexity of the feed, the difficulty of characterizing the reacting environment and the intricate hydrodynamics of the upgrading reactors [12, 13, 19, 20, 22, 23, 35, 36, 102-108].

$$\mathrm{Residue\ (A) + H_2 \rightarrow Non\ Residue\ (B)} \tag{3.1}$$

$$\mathrm{r_A = -k_A \rho_A \left(P_{H_2}\right)^{\beta}} \tag{3.2}$$

$$k_A = k_{A0}.\exp\left(-\frac{E_A}{RT}\right) \quad 3.3$$

The slurry hydrocracker is assumed to operate as an isothermal and isobaric single phase continuously stirred tank reactor. When combining equations 3.2 and 3.3 with a liquid phase mass balance on species A, the concentration and conversion of the residue can then be calculated for a given reactor volume in equations 3.4 and 3.5. The β, k_{A0} and E_A fitting parameters are determined in Microsoft Excel by minimizing the sum of squares for conversion data obtained at various temperatures, hydrogen pressures and LHSV (see Table 3.3) [72, 73]. The determination of the gas phase volumetric void fraction was based on correlations developed in Canmet report 77-48 [109].

$$\eta_A = \left[1 + k_A\left(P_{H_2}\right)^{\beta}\frac{V(1-\varepsilon)}{v_{AB_0}}\right]^{-1}\eta_{A0} \quad 3.4$$

$$X = 1 - \left[1 + k_A\left(P_{H_2}\right)^{\beta}\frac{V(1-\varepsilon)}{v_{AB_0}}\right]^{-1} \quad 3.5$$

The fitted results presented in Figure 3.4 are relatively accurate, with an absolute average relative error of ±3.37%, considering the simplifications and assumptions proposed for the hydrocracking model. Moreover, the F test value between the lack of fit and the pure error of the data is determined to be 0.7811. Since it is not larger than the critical $F_{5\%,64,7}$ value of 3.299, there is no significant lack of fit in the proposed model which makes it valid for the presented range of residue conversion.

Table 3.3: Hydrocracker model fitting parameters

Residue conversion

k_{A0}	-4.730E+15
E_A	2.097E+05
β	0.20

Product mass distribution ratio

	LE	NPH	LGO	HGO	VR
B_i	7.639E-03	5.023E-02	2.828E-01	6.585E-01	-1.000E+00
C_i	1.365E-01	8.064E-02	2.214E-01	-4.378E-01	2.361E-11

Hydrodesulfurization conversion

a	28.80
b	89.40
c	-26.23

Product sulfur distribution

	NPH	LGO	HGO	VR
a_i	414.66	2274.51	2.27	55.81
b_i	-368.60	-2074.19	25.29	40.28
c_i	86.88	557.39	14.41	-117.20
d_i	0.98	0.99	4.99	3.99

Light end composition

	C_1	C_2	C_3	C_4
a_i	14.91	17.64	37.97	29.48
b_i	-16.53	2.03	-30.43	44.93
c_i	10.73	-3.70	33.54	-40.57

The second section consists of modeling the mass yield distribution and hydrotreating conversions, based on results taken from an ebullated-bed hydroconversion experiment with Ni-Mo catalyst [76]. The data utilizing the least amount of catalyst were considered since, as mentioned, the iron additive present in the Canmet hydrocracker is not very catalytically active towards hydrogenation [4, 11, 35, 62, 76]. The reason why slurry hydroconversion data was not selected for the second section of the model is because there is no publicly available data from an experimental campaign that provides: (1) the petroleum product mass fraction distribution, (2) their sulfur and nitrogen content and (3) the heteroatom removal of the petroleum products produced from the hydroconversion of vacuum residue (b.p. 540+ºC) with a low-activity catalyst/additive.

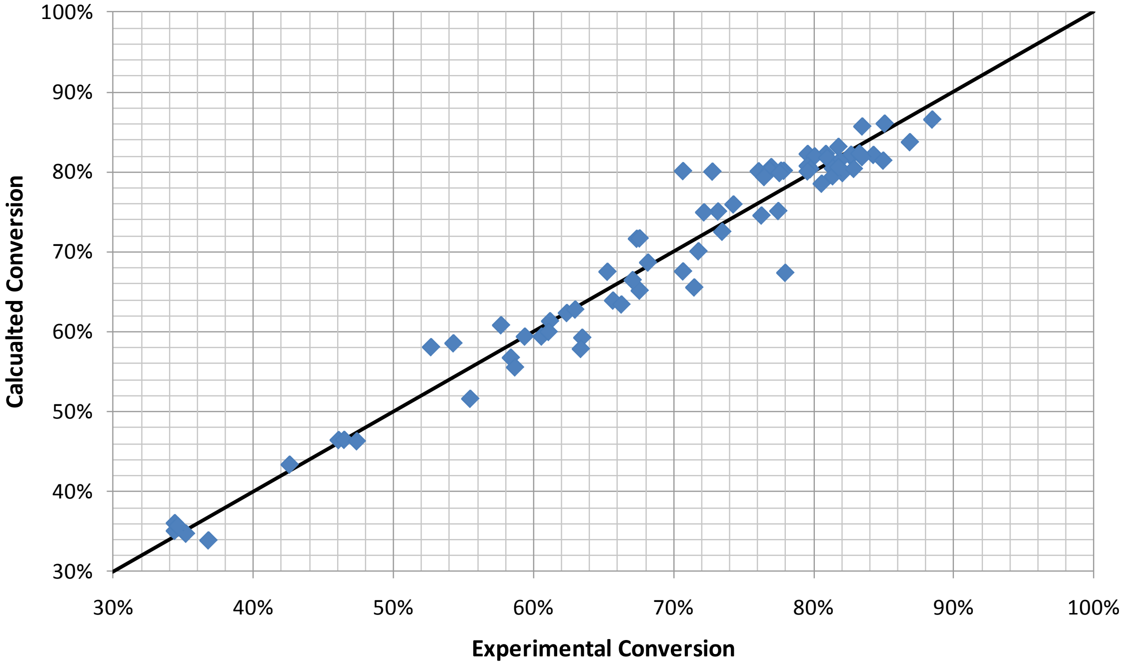

Figure 3.4: Fitting results of calculated versus experimental vacuum residue conversions

When cracking occurs in the heavy petroleum fraction, the lighter products are distributed according to the model presented in equations 3.6-3.8 [35, 36, 72, 106]. It is important to note that VR is not the only fraction that is cracked in the reactor; the HGO and/or LGO may also undergo scission but due to the limited data, a model could not be proposed for these reaction paths. However, the model does consider a decrease in the HGO fraction at higher conversion, a correction that allows the model to resemble the behavior of the hydrocracker reacting environment.

$$X = \frac{\eta_{A_0} - \eta_A}{\eta_{A_0}} \quad 3.6$$

$$\alpha_i = A_i X + B_i X^2 \quad 3.7$$

$$\eta_i = \alpha_i \eta_{A_0} + \eta_{i_0} \quad 3.8$$

The removal of sulfur is correlated with residue conversion in order to keep the model tied to the Canmet hydrocracker operation. Therefore, a change in temperature, pressure and LHSV impacts the VR conversion which in turn, causes the hydrodesulfurization conversion to vary (see equation 3.9, with data presented in Table 3.4). Removing nitrogen compounds from oil is generally more challenging than sulfur which is why it is sometimes neglected in hydroconversion models [4, 10, 11]. However, since the Canmet hydrocracker operates at high temperatures and contains fine metal catalyst, hydrodenitrogenation was assumed to be 60% of the hydrodesulfurization conversion, a value that should be between 30 to 80% [3, 6, 103, 110]. The hydrodemetallization conversion in slurry hydrocrackers is very high due to the abundance of a fine iron catalyst. Therefore, it is reasonable to assume a complete hydrodemetallization conversion during bitumen upgrading [111].

$$X_{HDS} = a + bX + cX^2 \quad 3.9$$

$$X_{HDN} = \text{Ratio}_{\frac{HDN}{HDS}} \left(a + bX + cX^2\right) \quad 3.10$$

After determining the amount of sulfur and nitrogen removed from the oil, it is necessary to estimate the amount of heteroatoms exiting in form of H_2S and NH_3 as well as the heteroatom redistribution in the hydrocracker petroleum total liquid product. The distribution of sulfur and nitrogen is dictated by a linear regression in function of residue conversion, expressed in equation 3.11. The equation is based on residue conversion instead of temperature, pressure and LHSV in order to link the Canmet slurry hydrocracker model with the product distribution. The light hydrocarbon distribution of the petroleum product, ranging from C_1 to C_4, is modeled with equation 3.12.

Table 3.4: Effect of pressure, temperature and LHSV on the residue conversion and sulfur removal at 1wt% Ni-Mo catalyst content in an ebullated-bed reactor [76]

Temperature (°C)	LHSV (h-1)	Pressure (MPa)	Residue Conversion (%)	Sulfur Removal (%)
410	0.5	16	27.8	51.8
420	0.5	16	45.1	61.2
430	0.5	16	61.6	70.5
440	0.5	16	77.5	80.7
450	0.5	16	92.7	91
430	0.25	16	88.7	84.8
430	0.38	16	74.7	77.4
430	0.5	16	61.6	70.5
430	0.63	16	50.9	65.4
430	0.75	16	40.9	60.9
430	0.5	12	62.4	69.1
430	0.5	14	62.1	69.8
430	0.5	16	61.6	70.5
430	0.5	18	60.4	71.2
430	0.5	20	59	71.9

$$\mathrm{\gamma_i = a_i.\ln(X + d_i) + b_iX + c_iX^2} \tag{3.11}$$

$$\mathrm{LE_i = a_i + b_iX + c_iX^2} \tag{3.12}$$

The hydrogen consumption of processes dealing with sour heavy petroleum is relatively high mainly due to the extensive cracking and treating occurring [4]. Moreover, some of the hydrogen is absorbed and lost in the liquid products while the rest is flashed in equilibrium with the light ends. The remaining hydrogen losses are contingent on the efficiency of the hydrogen separation method and amount purged during the recycle. For the purpose of this model, the hydrogen consumption estimated is completely utilized in hydrogenation. Since the hydrogen consumption was not registered in the data, equation 3.13 approximates its value based on residue conversion, with a maximum utilization of 2000 scf H_2/bbl oil [3, 5, 7, 112].

$$\text{Total } \mathrm{H_2} \text{ consumed } \left(\frac{\mathrm{scf}}{\mathrm{bbl}}\right) = 2000.\mathrm{X} \tag{3.13}$$

The last step of the model is to distribute the hydrogen amongst the product. The lighter petroleum fractions contains a higher hydrogen percentage than the heavier ones [113]. Consequently, a product C to H ratio redistribution is necessary in order to satisfy the hydrogen and carbon mass balance.

The Aspen HYSYS® hydrocracker model (see Figure 3.5) is implemented in a sub-flowsheet where calculations were performed in the simulator spreadsheet interface and linked to a Petroleum Shift Reactor present in the Refinery Operations. A dynamic alternative consists of integrating the Petroleum Shift Reactor to a user unit operation customized in the VBA environment. The light ends, NPH, LGO, HGO and non-converted hydrocracker residue blended product are fractionated in a distillation section after which every fraction except the hydrocracker residue are sent to their respective hydrotreating unit for further processing. The distillation tower is a Aspen HYSYS Petroleum Refining distillation model that fractionates a petroleum blend into products based on boiling point distribution and calibration parameters [48]. The unit solver is therefore affected by calibration factors that are adjusted based on operating parameters and the extent of separation required.

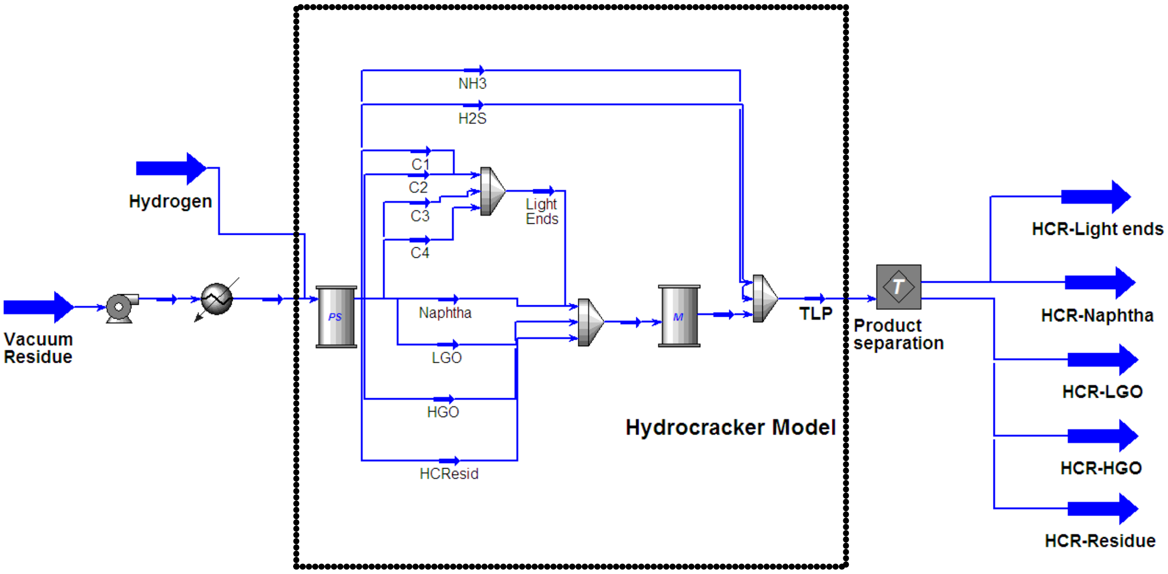

Figure 3.5: Aspen HYSYS® Canmet slurry hydrocracker model implementation

3.4. __Hydrotreating__

The hydrotreating reactors are vessels that upgrade the separated NPH, LGO and HGO originating from the distillation towers and slurry hydrocracker. The NPH hydrotreater processes petroleum blends with true boiling points below 180ºC. It operates at a temperature of 280ºC and a pressure of 3.2 MPa. The LHSV of the reactor should remain close to 5 h^{-1} with a H_2/Oil ratio of 400 scf/bbl [4, 92, 99]. The LGO hydrotreater is operated at a temperature of 310ºC, a pressure of 5.6 MPa, a LHSV of around 2.5 h^{-1} and a H_2/Oil ratio of 800 scf/bbl, dealing with petroleum fractions between 180-360ºC. The HGO has the most severe reaction environment of the three hydrotreaters since it deals with petroleum fractions ranging between 360-540ºC and a reactor temperature of 360ºC, pressure of 12 MPa, a LHSV ranging between 1-1.5h^{-1} and a H_2/Oil ratio of around 1200 scf/bbl.

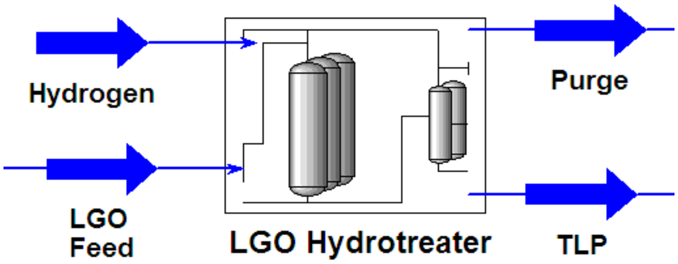

Figure 3.6: Aspen HYSYS® LGO hydrotreater model

The three hydrotreaters are simulated similarly in a hydrocracker reactor model provided in the Aspen HYSYS Petroleum Refining package (see Figure 3.6). The reactors are calibrated to achieve an average hydrodesulfurization and hydrodenitrogenation conversion of around 90% and 72%, respectively, while minimizing the hydrocracking reaction. The reactor feed has to be correctly characterized in order to accurately convert the Aspen HYSYS® feed to the Aspen property databank that the hydrocracker model uses. The feed conversion libraries had to be modified for the NPH and HGO feeds since the feed types characterization parameters provided by AspenTech were inapplicable. The library has the task of typifying petroleum properties such as density, molecular weight, aromaticity, boiling point distribution and sulfur and nitrogen content in 89 different characteristic hydrocarbon molecules. However, the provided libraries are not equipped to handle high heteroatom feeds that vary significantly from crude and middle range hydrocarbons. Therefore, the construction of adapted libraries was necessary for which the difference between the initial Aspen HYSYS® and the estimated hydrocracker environment petroleum properties was minimized. The monitoring of the mass and energy balances of the reactors is necessary in order to avoid discrepancies resulting from the feed library conversions.

3.5. Results and discussion

The bitumen upgrading process simulation contained a distillation section, three hydrotreaters and a hydrocracker to ultimately form a high quality SCO. The utilities consumption associated to these units are presented in Figure 3.7. The utility consumption of the DRU and vacuum distillation tower were determined in Aspen HYSYS® and verified with correlations from other crude refining and upgrading processes [7, 99], whereas the hydrotreaters and hydrocracker's fuel, cooling water and steam requirements were estimated based on similar upgrading process units available in the "*Refining Processes Handbook"* [99]. However, the total electrical consumption of the hydrotreaters and hydrocracker was determined based on the power demand of the hydrogen compressor and the upgrader petroleum feed pumps. The hydrogen recycle and quench ratio is assumed to be 4-7 times larger than the hydrogen consumption of the units [99]. The calculated electrical consumption of the upgrading process is 71.73 MW whereas a 350,000 BPD of SCO upgrading facility operated by Syncrude Canada Ltd. requires a utility plant that provides 350 MW of power [114, 115]. The distillation towers are the units that deal with the highest oil flow rates which explain their higher demand in utilities. However, the hydrocracker is the unit that utilizes the most utilities per feed rate because it has the highest operating pressure and temperature in the upgrading process. The utility consumption calculations assume that the petroleum product of each upgrader is separated into pseudo-components in case subsequent refining is required which conservatively overestimates the most utility consumption.

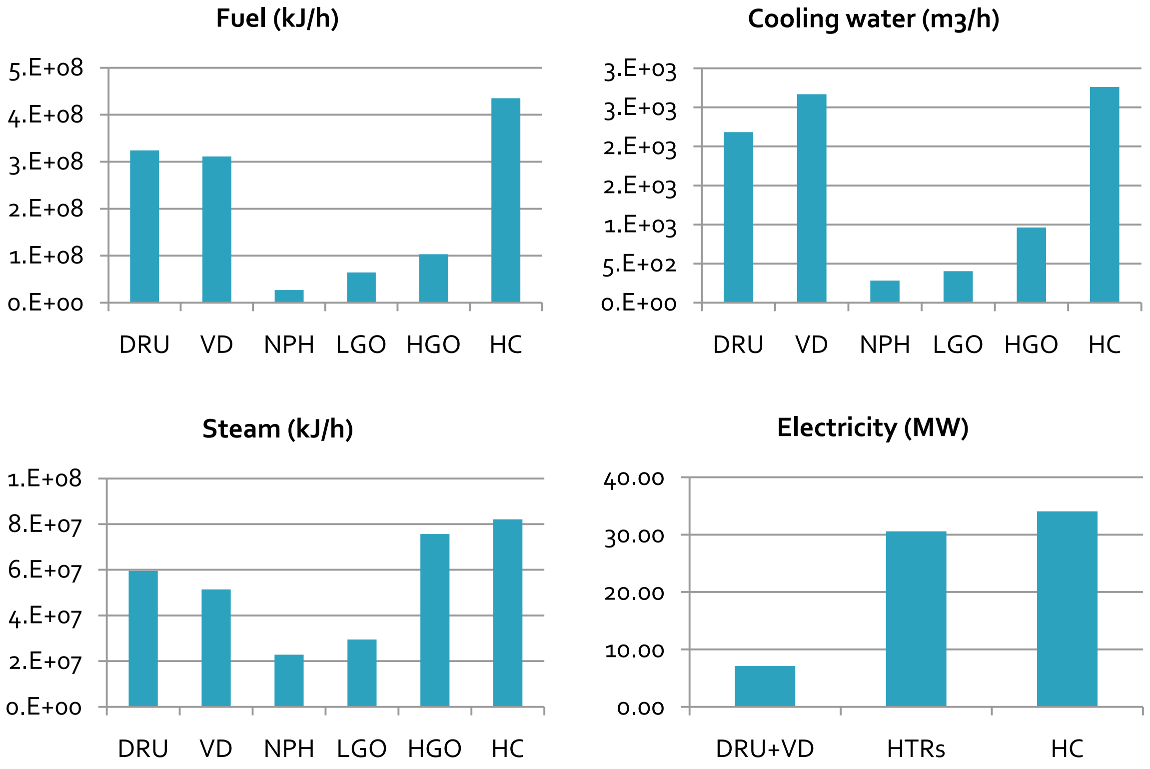

Figure 3.7: Utilities consumption of the main process operations [7, 99]

Since the upgrading technologies consume large amounts of hydrogen, it is important to determine the necessary H_2 requirements and its sensitivity to major operating parameters change. A case study is performed in which the hydrocracker is operated at a constant pressure of 17.89 MPa and a LHSV of 0.48h^{-1} while the temperature is varied between 420-460ºC, which increases residue conversion. From Figure 3.8, a rise in hydrocracker conversion leads to an increase in hydrogen consumption in the hydrotreaters due to the higher flow rate of <540ºC compounds. Nonetheless, it is insignificant compared to the hydrocracker's increase in

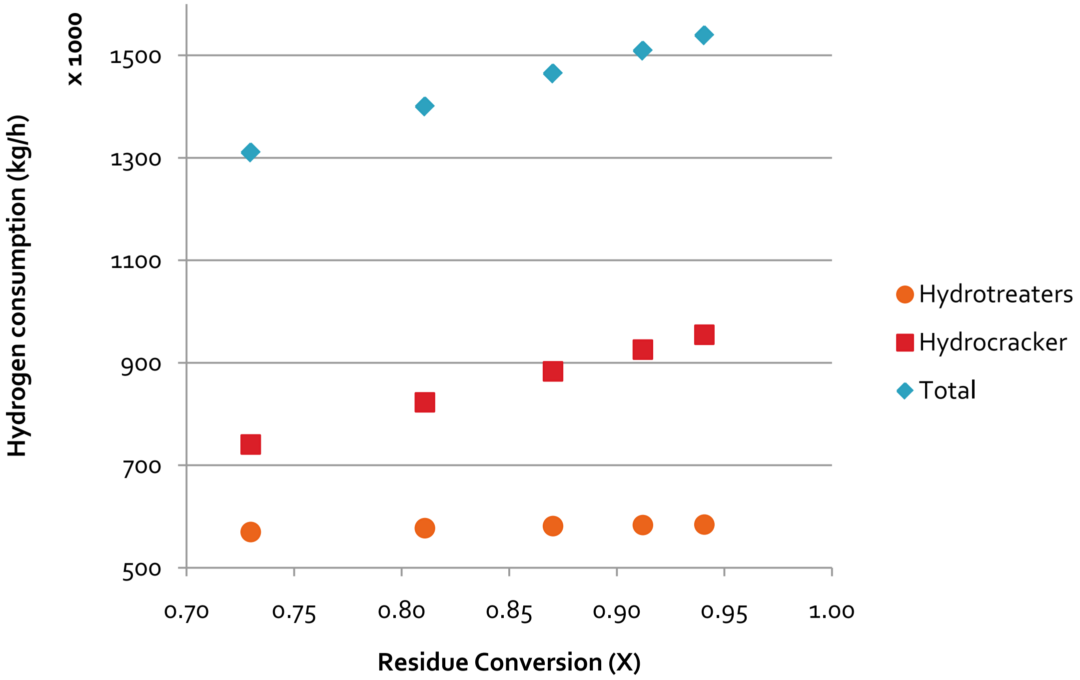

Figure 3.8: Hydrogen consumption of the hydrotreaters, the Canmet hydrocracker and the total upgrading process

hydrogen demand which is 10 to 15 times larger. The hydrotreating hydrogen demand is primarily contingent on its feed flow rate since its operation is generally maintained to reach 80-95% hydrodesulfurization and 60-75% hydrodenitrogenation.

The hybrid hydrocracker model predicts accurate residue conversions for a Canmet slurry hydrocracker but the product mass yields and hydrotreating conversions are based on an ebullated-bed reactor data with Co-Mo catalyst operating in a generally less severe environment. As a result, the change in catalyst and reaction conditions has an impact on the hydrotreating, hydrogenation and middle distillate selectivity. The Canmet slurry hydrocracker product should have a greater fraction of light ends and NPH than the characterized product of the hybrid model (see Figure 3.9) and as a result, a residue with higher carbon content.

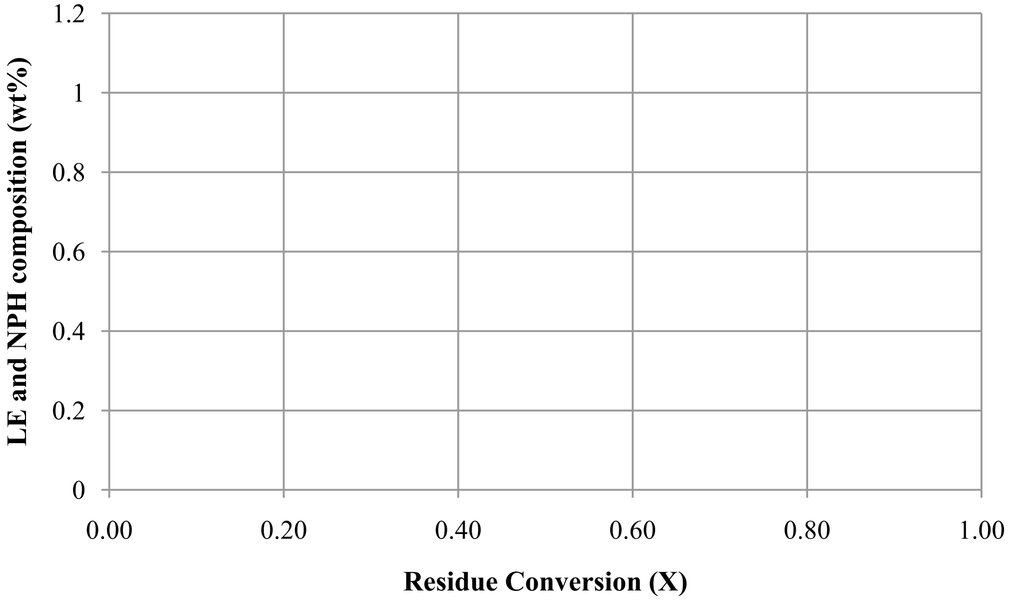

Figure 3.9: Combined light ends and NPH products mass wt% in function of residue conversion comparing the experimental data (dotted) with the model estimation

The hybrid model calculation of lower light end and NPH yields leads to an overestimate of the hydrogen consumption. In the upgrading process, the hydrogen demand is reduced when less middle distillates are produced since NPH utilizes lower amount of hydrogen for hydrotreating than LGO and HGO. However, the hydrogen demand of the hydrocracker should also be affected by the total liquid product selectivity but for the purpose of this model, it was determined to be function of the residue conversion only. Therefore, the hydrogen consumption is conservatively estimated with a consumption maximum of 2000 scf/bbl, in order to always meet the hydrogen requirements of the process with a potential excess.

The produced SCO quality is dependent on the hydrocracker and hydrotreating conversions. Its API gravity and sulfur content are generally the parameters used in the valuation of the SCO price [116]. However, in order to correctly simulate the industrial operation of the units, their conversions should be maintained at their optimal point. For a hydrocracker residue conversion of 91% and an average hydrotreating desulfurization and denitrogenation of around 90% and 72%, a SCO with a sulfur content of 0.164wt%, a nitrogen content of 0.066wt% and an API gravity of 27.71° is obtained. Since the hydrocracker residue is not combined with the produced SCO, the product volumetric yield is 97.1% with regards to the bitumen; however the value increases beyond 101.2% if the residue is recycled back to the hydrocracker or mixed with the final product. The elevated hydrodesulfurization, hydrodenitrogenation and light end formation contribute to the reduction of the volumetric yield of the product. The required hydrogen consumption for this operation is equal to $1.52*10^4$ kg/h. For a lower quality SCO with 0.485wt% sulfur and 0.1wt% nitrogen, 20.6% of the hydrotreater feed should be by-passed which causes the product's API gravity to drop to 26.8° and the total hydrogen consumption to be reduced by 7.96%.

Since the SCO does not contain the hydrocracker residue, that high boiling point and carbonaceous fraction can be upgraded further in a coker to produce more light oils, burned in cement kilns and boilers or charged in a gasification process for hydrogen production. Since the hydrocracking and hydrotreating reactions consume over 15,000 kg/h of hydrogen, the process could be integrated with a gasification process in order to reduce the net hydrogen demand, with the possibility of H_2 self-sufficiency. The entrained flow gasifiers handle various types of feeds and some may benefit from the presence of iron which can potentially reduce slag viscosity if high levels of conversion and non-hazardous solid products are desired, thus allowing the reactor to operate at a lower temperature [27, 49, 50]. The introduction of gasification is also beneficial since the heteroatom and toxic compounds present in the residue can be captured. For example, an acid gas removal section, e.g. amine process, Rectisol and Selexol, can remove CO_2 and H_2S

from gaseous streams. The bitumen upgrading and gasification integrated process emissions can be calculated and optimized in order to meet environmental regulations while supplying sufficient amounts of hydrogen to the hydrocracker and hydrotreaters. The emissions of CO_2 during the production of SCO via surface mining and upgrading are estimated at 62-164 kg CO_2/bbl SCO while in-situ methods, such as SAGD, and upgrading emit 99-176 kg CO_2/bbl SCO [117-119]. Since the simulated process produces around 97,000 barrels of SCO per day, the average CO_2 emission for mining and in-situ methods followed by an upgrading facility is 3.997 and 4.864 million tonne per year, respectively.

3.6. Conclusion

The simulation of a 100,000 BPD Athabasca bitumen upgrading facility utilizing the Canmet slurry hydrocracking process requires around 1,265 GJ/h of heating fuel, 9,259 m^3/h of cooling water, 321 GJ/h of steam and 71.73 MW of electricity. The process was simulated in Aspen HYSYS® and contains a desalter, DRU, vacuum distillation, hydrocracker and three hydrotreaters (NPH, LGO and HGO). A hybrid hydrocracker model was developed to predict the residue conversion utilizing Canmet data and then estimate the products mass yields and extent of hydrotreating reactions based on data from a low catalyst load ebullated-bed reactor. The hydrogen consumption of the proposed model is conservatively overestimated at a value of $1.52*10^4$ kg/h since the products yield have a smaller than expected fraction of gas and NPH and thus a greater quantity of LGO and HGO, which require more hydrogen for downstream hydrotreating. Operating the Canmet hydrocracker at 450ºC, 17.89 MPa, and a LHSV of 0.48 h^{-1} results in a residue conversion of 91%. The operation of the hydrotreaters allows an average hydrodesulfurization/hydrodenitrogenation conversion of 90/72% for which a SCO is produced with a sulfur and nitrogen content of 0.164 and 0.0656wt%, respectively. The SCO volumetric yield is 96.85%, however it can be augmented beyond 101.3% if the residue is recycle back to the hydrocracker or mixed with the final SCO product. Nonetheless, the proposed upgrading process residual hydrocracker residue has the potential to be integrated into a gasification process from which hydrogen can be extracted. The iron based catalyst present in the residue makes the integration with an entrained flow slagging gasifier attractive since the metal has the potential to reduce the slag viscosity and resulting oxygen demand. The option of carbon capture can also be implemented in the integrated simulation. The upgrading process emits an estimated 3.997–4.864 million tonne/year of CO_2 for a 100,000 BPD extraction/mining and upgrading process.

4. Simulation of the Integration of a Bitumen Upgrading Facility and an IGCC Process with Carbon Capture

4.1. Introduction

The worldwide oil demand is on the rise and is predicted to climb from around 85 to 105 million barrels per day by 2030 [1]. Unconventional oil resources, i.e. extra heavy oil and bitumen, consist of around 6 trillion barrels which constitutes about 30% of world oil reserves [91, 120]. However, before refining, the unconventional oil requires upgrading via carbon rejection or hydrogen addition technologies due to their high heteroatom content, viscosity, boiling point and density. The simulation of a bitumen upgrading process operating with unit operations including a Canmet slurry hydrocracker and naphtha (b.p. 40-180ºC) hydrotreater, light gas oil (b.p. 180-360ºC) hydrotreater and heavy gas oil (b.p 360-540ºC) hydrotreater was performed using Aspen HYSYS® in order to determine the hydrogen consumption of the facility, CO_2 emitted, utility consumption and quality of synthetic crude oil (SCO) based on various operating parameters. The residue (b.p. 540+ºC) withdrawn from the slurry hydrocracker could be subsequently upgraded in a coker in order to produce more light oils, burned in cement kilns and boilers or charged in a gasification process for hydrogen production [2]. The upgrading simulation estimated a hydrogen requirement of 15,000 kg/h for the production of a high yield high quality SCO from 100,000 BPD of Athabasca bitumen [121]. In order to reduce the net hydrogen requirements, the hydrocracker residue can be integrated with a gasification facility.

Similar upgrading process combinations have been tested or contemplated industrially. The Long Lake integrated upgrading project operated by Nexen Inc. charges deasphalted bottoms in four Shell Gasification Process trains in order to ultimately produce the required hydrogen for their hydrocracking operation and for syngas fuel that can be utilized for SAGD or cogeneration (Cogen) operations [29, 93]. The North West Upgrading Inc. facility is an ongoing project that plans to combine the LC-Fining technology and a heavy petroleum residue gasifier [94]. The Shell Pernis Refinery in Rotterdam, Netherlands also includes a gasification process in their plant in order to produce synthetic gas from heavy visbreaking residue or straight-run vacuum residue [31]. The bitumen upgrading and gasification process integration have additional potential benefits than solely alleviating the hydrogen demand of the hydrocracker and hydrotreaters and maximizing the SCO volumetric yield. The addition of acid gas removal technologies such as amine, Rectisol or Selexol for CO_2 and H_2S capture allow the overall process to reduce criteria for air contaminants and CO_2 emissions. The inclusion of high hydrogen syngas gas turbines and steam turbines can also allow the plant to potentially achieve power and thermal self-sufficiency. In this study, the effect of 65% and 90% carbon capture cases has been evaluated relative to the integrated process operation without carbon capture and the amount of gasifier feed required to meet the upgrading process hydrogen demand is estimated for various hydrocracker residue conversions.

4.2. <u>Process description and simulation</u>

The overall process presented in Figure 2.3 consists of the integrated Athabasca bitumen upgrading facility and the gasification process studied here. The upgrading section residue is fed to a gasifier in which carbon monoxide and hydrogen are produced forming a synthetic gas called syngas. The syngas is cleaned and cooled prior to the removal of sulfur species. The sweet syngas is then passed through water-gas shift reactors in which carbon monoxide and water react to produce hydrogen and carbon dioxide. Pre-combustion carbon capture via a MEA solvent increases the syngas hydrogen concentration in order to appropriately recycle a portion of the stream to the hydrocracker and hydrotreaters while directing any excess gas to the combustion and steam turbines. The steam and power produced supply the gasification process electrical and thermal requirements thus necessitating a hydrogen stream large enough to satisfy that condition.

The process simulation is performed using Aspen HYSYS®, which is equipped with a strong thermodynamic foundation and a variety of property packages. Containing over 1,000 pure components, Aspen HYSYS® has the option to create hypothetical compounds and assist the user in defining crude oil assays in its Oil Environment where oil properties and characteristics can be specified or estimated with several embedded correlations. For the simulation of the gasification section, the PRSV (Peng-Robinson-Stryjek-Vera) thermodynamic model is chosen which consists of a modified PR model with an improved characterization of vapour pressures of pure components and their mixture [44, 46, 47, 98].

4.2.1. Air Separation Unit

Oxygen for gasification and sulfur recovery are provided by a cryogenic air separation unit (ASU) [80, 122]. Operated at temperatures below -185ºC, the ASU separates ambient air into a 95mol% oxygen rich stream and a nitrogen stream exceeding 99mol% purity. The inlet air is processed for the removal of particulates before compression in a multistage intercooled centrifugal compressor. Water, CO_2 and saturated hydrocarbons are subsequently removed to avoid precipitation due to cryogenic temperatures. 70% of the compressed air is fed directly into the cold box while the rest is compressed by an air booster and cooled further before injection, as proposed by the DOE/ NETL [80]. The air feed is cooled to cryogenic temperature before distillation by the separated products of the cold box. The separated nitrogen is compressed and fed to the gas turbine as dilution gas whereas the excess nitrogen is sent into a turbo expander before being released into the atmosphere. Likewise, the separated 95mol% oxygen is compressed and fed to the gasifier and Claus sulfur recovery burner while controlling the air feed flow in order to meet the gasification oxygen demand. The ASU compressors are powered by electric motors for which the power consumption is determined at a polytropic efficiency of 85%.

4.2.2. Gasification

An entrained flow slagging membrane wall gasifier is proposed for the handling of the hydrocracker residue because of its capability to gasify a variety of feedstocks including coals, ranging from bituminous coal to lignite, petroleum coke and heavy petroleum blends [50, 123]. The gasifier converts carbon feeds into carbon monoxide and hydrogen by adding oxygen and/or steam [49-51, 77]. The entrained flow slagging gasifier operates above ash melting temperatures which are generally over 1300ºC, depending on the feed, and at pressures of 20-70 bar. The gasifier temperature is controlled by raising high pressure steam in the reactor shell while assuming a heat loss of around 0.65% of the fuel's HHV [44, 77, 80, 124, 125]. Moreover, the hydrocracker residue contains a high iron content due to the addition of iron-based catalyst which can potentially reduce the slag viscosity and the ash melting point and consequently, the reactor operating temperature [27, 28, 126, 127]. Figure 4.1 presents slag liquidus projections for a Canmet hydrocracker residue. Considering the top point of the triangle as an iron-free residue, it can be observed that the slag melting point diminishes as the iron content increases while moving down the right-hand side. Moreover, the figure illustrates that the presence of iron

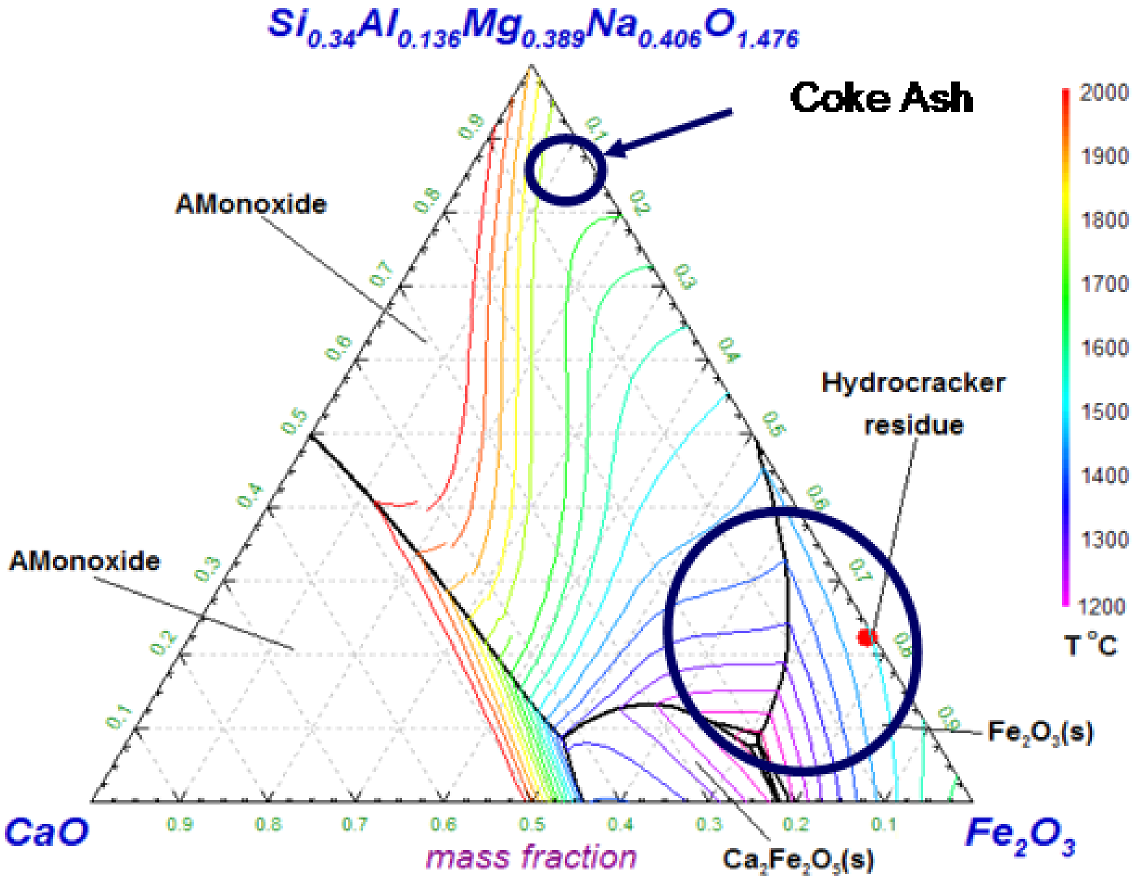

Figure 4.1: Slag liquidus projections for hydrocracker residue [27, 28]

and calcium oxides can act as network modifiers since the addition iron can reduce the liquidus slag forming temperature of the Canmet hydrocracker residue to 1500ºC. With the addition of a small amounts of CaO as a fluxant, the gasifier operating temperature can be potentially reduced to 1300ºC [27, 28].

The mass fraction and heat of combustion of the hydrocracker residue obtained in Aspen HYSYS® has been compared with a Canmet slurry hydrocracker laboratory sample shown in Table 4.1. The hydrogen to carbon molar ratio of both samples is around 1.45 which validates the simulation hydrocracker product. An elemental analysis definition approach is utilized to characterize the feed in Aspen HYSYS®, however discrepancies are observed when comparing the residue combustion heat values. The simulation estimates a HC residue higher heating value (HHV) of 42.81 MJ/kg while the laboratory data specifies a value of 41.10 MJ/kg. Therefore, when assuming an ash fraction of 2.18wt%, approximately 4% of the fuel mass flow has to be removed from the gasifier feed and reinserted in the syngas. This modification allows the HHV of the feed to be reduced to the experimental sample data. If more power and steam is required, petroleum coke can also be co-fed into the gasifier and has to be characterized and corrected similarly.

Table 4.1: Hydrocracker residue and petroleum coke mass compositions

	HC Residue (HYSYS)	**HC Residue (#10472-01)**	**Cold Lake Petroleum Coke [11]**
Carbon	85.61%	83.40%	82.19%
Hydrogen	10.36%	10.10%	5.54%
Sulfur	2.42%	3.50%	7.63%
Nitrogen	1.61%	0.82%	1.78%
HHV (MJ/kg)	42.81	41.1	28-31

The entrained flow slagging gasifier is simulated as a Gibbs reactor [44, 128, 129] which assumes that the gaseous product is at chemical equilibrium. The carbonaceous hydrocracker feed is charged into the reactor with 0.1 mole of steam and 0.45 mole of oxygen per mole of carbon (see Table 4.2). The syngas gasifier outlet is assumed to be the product of a carbon conversion of 99.5%, with the unconverted fraction exiting with the slag. The syngas is cooled to 890ºC with a 205 ºC syngas recycle stream. Subsequently, additional syngas cooling occurs in a radiant syngas cooler and raises more HP steam [80].

Table 4.2: Operating parameters of the gasifier and syngas molar composition

Gasifier operation

Temperature (ºC)	1427
Pressure (bar)	42
Ash content in pitch (wt%)	2.18
O_2/C (mole basis)	0.45
Steam/C (mole basis)	0.10
Reactor shell HPS/C (kJ/kmole)	54,351
Radiant cooler HPS/syngas (kJ/Nm^3)	814.8
Recycle syngas/hot syngas	0.853
Slag produced/C feed (kg/kmol)	0.481

Syngas molar composition

CO	63.88%
Hydrogen	31.17%
H_2O	0.26%
CO_2	0.14%
H_2S	2.10%
Argon	1.20%
Nitrogen	0.87%
Methane	0.37%
COS	0.01%

4.2.3. Acid gas removal

Due to the high heteroatom content of hydrocracking residue, the syngas has to be sweetened and treated. Acid gas removal (AGR) consists of removing environmentally hazardous molecules like CO_2, H_2S and COS. The total sulfur content in the syngas has to be reduced to very low concentrations since the CO water-gas shift occurs in a sweet WGS reactor. Consequently, it is also important to remove sulfur traces such as COS to avoid catalyst poisoning issues [78, 80].

The COS hydrolysis reaction is simulated isothermally at a temperature of 177ºC during which 99.5% of the COS has been converted into H_2S (see Table 4.3) [80]. In case of high mercury content, the simulation of activated carbon beds which can remove up to 95% is added following the COS hydrolysis reaction, at a temperature of 39ºC.

The MEA chemical absorbent is the most widely used type of solvent for the removal of H_2S and CO_2 from natural gas streams and was chosen for the purpose of the non-selective AGR section [83]. MEA solutions rarely exceed 30 wt% in order to avoid corrosion problems [84]. H_2S and CO_2 are non-selectively and reversibly removed with the amine solvent while COS irreversibly reacts with the solvent which results in solution loss in the system and validates the implementation of a COS hydrolysis reactor prior to amine treatment [83].

The Aspen HYSYS® simulation of the AGR process is optimized for high separation and low energy consumption and verified with design heuristics from the GPSA data book [83]. The Amines Property Package selected is the only thermodynamic package that can manage the simulation of the amine components present in the basis environment of the simulator [44, 130]. The Kent & Eisenberg equilibrium solubility model is selected which is valid over the range of 30ºC to 125ºC. The Amines Property Package is incompatible with some components present in the system, such as argon. In order to carry on with the simulation, the component has to be temporarily removed from the AGR flowsheet then re-added to the sweet gas stream after a transition in thermodynamic packages. The lean MEA solution has a concentration of 30wt% and contacts the sour gas in an absorption column. The AGR process lowers the H_2S concentrations to concentrations below 1 ppmv in order to avoid catalyst poisoning in the sweet WGS section

Table 4.3: Operating parameters of the COS hydrolysis reaction and the amine process

COS hydrolysis

CO hydrolysis reactor temperature (ºC)	177
CO hydrolysis conversion (%)	99.5

H_2S amine separation

Lean MEA concentration (wt%)	28.75
Acid gas pickup, (mol/mol MEA)	0.3401
Rich solution acid gas loading (mol/mol MEA)	0.5413
Reboiler heat duty (kJ/kg of amine)	282.9
Reboiler temperature (ºC)	126.8
Regenerator trays	12
Make-up water (g/kg of lean amine)	0.61

CO_2 amine separation

Lean MEA concentration (wt%)	28.92
Acid gas pickup, (mol/mol MEA)	0.4460
Rich solution acid gas loading (mol/mol MEA)	0.6189
Reboiler heat duty (kJ/kg of amine)	291.2
Reboiler temperature (ºC)	118.8
Regenerator trays	12
Make-up water (g/kg of lean amine)	1.472

downstream [78, 131]. A second pre-combustion carbon capture AGR section is also simulated with similar design parameters as the sulfur removal section. However, the solvent recirculation is going to be much larger because of the substantially higher concentrations of CO_2 present in the syngas which demands a significant amount of reboiler heat for solvent regeneration. It is desirable to maintain the AGR solvent loading capacity between 0.3-0.35 moles of acid gas per mole of amine to avoid equipment corrosion [83]. However, the CO_2 section is operated with a loading capacity of 0.446 moles of CO_2 per mole of amine in order to reduce reboiler duties.

4.2.4. Water-Gas Shift

The Water-Gas Shift is a chemical reaction that converts CO and H_2O to an equivalent amount of hydrogen and CO_2 as shown in equation 4.1.

$$\mathrm{CO} + \mathrm{H_2O} \rightarrow \mathrm{CO_2} + \mathrm{H_2} \tag{4.1}$$

Since the WGS reaction is exothermic, its equilibrium constant decreases with increasing temperature meaning that high CO conversion can only be achieved at lower temperatures. However, the reaction is faster at more elevated temperatures which is why sweet WGS reactors in series are designed with a high-temperature shift reactor (HTS) operating for fast CO conversion, followed by a low-temperature shift (LTS) unit for an increase in overall conversion. Some processes can also include a second LTS reactor for even higher CO conversions. Due to the exothermic nature of the reaction, the HTS and LTS reactors outlet temperature can be controlled by a direct water quench or by an indirect inter-cooling system. The HTS reactor's excess heat is captured in intermediate pressure (IP) steam while the LTS reactor outlet temperature is used to preheat the pre-combustion hydrogen-rich syngas.

WGS is a crucial step in the proposed bitumen upgrading and gasification integration during which hydrogen is produced. The WGS reaction specifications are selected from a defined Aspen HYSYS® reaction library. Due to its equilibrium nature, its conversion is greatly impacted by the amount of water fed. A product steam-to-dry gas (S/DG) molar ratio of 0.25 has been chosen for the sequence of HTS and LTS reactors in order to reach a CO conversion of 94.76%, while assuming a 95% equilibrium approach (see Table 4.4) [78]. The steam ratio has an impact on equilibrium but also affects the overall power production of the process since it consumes high quality steam from the heat recovery steam generation (HRSG) unit. Conversely, if lower conversions are achieved, more steam will be available for power production but less hydrogen will be produced for the upgrading process and gas turbine. A lower conversion also reduces the efficiency of the pre-combustion CO_2 capture process due to the low reactivity and solubility of unreacted CO with the amine solvent [78, 80, 132, 133].

Table 4.4: Operating parameters of WGS and product mole fraction

WGS operating parameters

HTS feed temperature (ºC)	310.0
HTS product temperature (ºC)	540.0
LTS feed temperature(ºC)	180.0
LTS product temperature (ºC)	272.1
Product steam to dry gas ratio (mole basis)	0.25
Steam to CO ratio (mole basis)	1.565
MP steam produced (kJ/Sm^3 syngas)	429.8
HTS CO conversion (%)	68.52
LTS CO conversion (%)	83.34
Overall CO conversion (%)	94.76

Syngas molar composition

Hydrogen	46.40%
CO_2	30.63%
H_2O	20.04%
CO	1.69%
Argon	0.61%
Nitrogen	0.44%
Methane	0.19%

4.2.5. Combustion turbine

The gas turbine generator, i.e. combustion turbine, selected for the high hydrogen combustion gasification process is based on the advanced F Class turbines. The unit consists of an axial flow, single spool and constant speed machine with a controllable inlet guide vane. Furthermore, the gas turbine contains advanced bucket cooling techniques, superior alloys and compressor aerodynamics that allow higher firing temperatures to be reached. The F Class turbines (e.g., GEE7FB) are assumed to be commercially available for conventional and high hydrogen content syngas [80, 96, 134].

The simulation of the combustion turbine was separated into three parts (see Figure 4.2); (1) feed pre-treatment, (2) combustion chamber design and (3) hot flue gas expansion. The hydrogen-rich syngas is distributed between the bitumen upgraders and power generation units. The upgrading facility recycle hydrogen is preheated and compressed to the required operating conditions. If the amount of carbon capture is not maximized and the hydrogen content of the recycle stream is reasonably low (below 90 mol%), then the addition of a pressure-swing adsorption unit is necessary [4, 5, 7, 10]. The residual hydrogen split is preheated with the hot LTS product before being utilized for power generation. A specific amount of dilution nitrogen provided by the ASU is necessary to regulate the LHV of the syngas and the turbine inlet temperature (TIT). Since the net syngas stream is reduced due to the upgrading facility hydrogen recycle, the nitrogen could be in excess. The surplus should therefore be charged through a turbo expander for supplementary power generation. A specific amount of oxygen is also required for syngas combustion. Therefore, air is compressed and injected with the diluted syngas into the combustion chamber, which is simulated as a Gibbs reactor. The hot outlet gas is then injected in a series of turbines. It is important to note that the overall power generated in the combustion turbine satisfies the power requirements of the air compression provided by the attached single spool compressor.

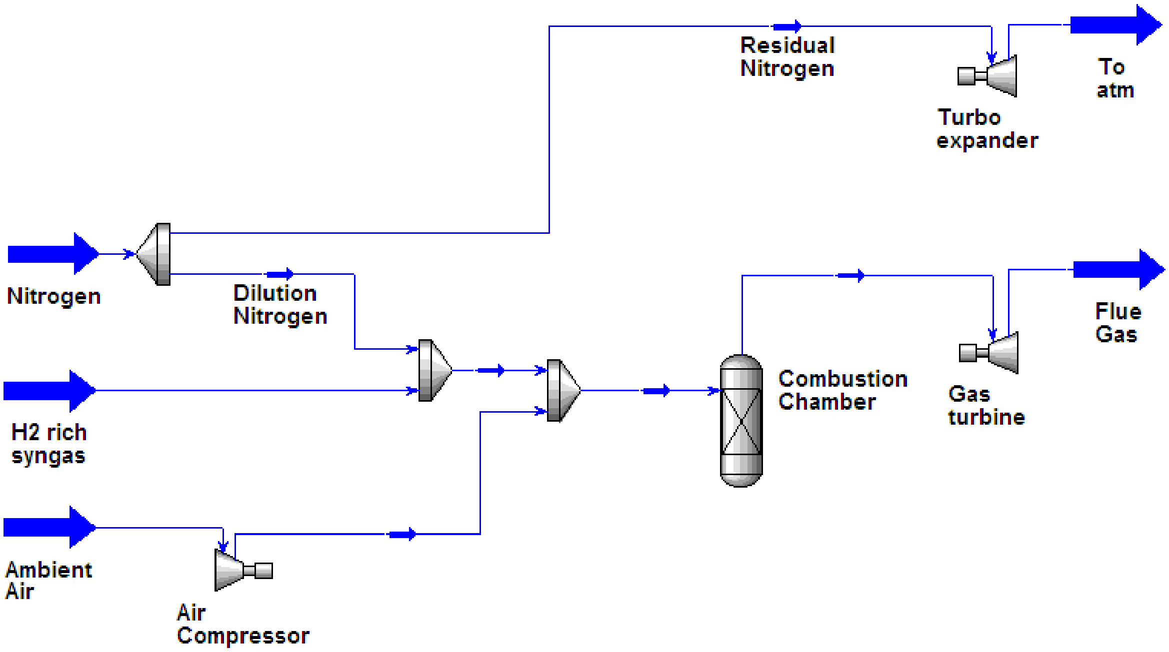

Figure 4.2: Simplified flowsheet of the simulated gas turbine section

The turbine inlet temperature is a very important parameter in IGCC power generation. The thermal efficiency of the process increases with higher TIT which is why the gas turbine manufacturers attempt to constantly increase the thermal tolerance of their turbines by improving their construction material and design [87, 135]. For the purpose of the Advanced F Class turbine, the TIT is defined as 1371ºC for natural gas combined cycle. However, for a high hydrogen system IGCC with carbon capture, the inlet rotor temperature is specified to be 1317-1322ºC. Since high hydrogen carbon capture cases have high water contents flue gases, i.e. 12.74mol%, the TIT is reduced in order to conserve the equipment. High hydrogen gas turbine combustors have to be evaluated carefully by the manufacturer due to the high flame speeds that can cause a flashback or primary zone re-ignition. Following combustion, the hot flue gas is expanded in a three stage turbine expanders to a minimum temperature of 564ºC. The flue gas pressure should not drop below 1.1 bar in order to overcome the heat recovery steam generator (HRSG) pressure drop [80, 134, 136].

4.2.6. Heat Recovery Steam Generator

A typical HRSG is described as a "horizontal gas flow, drum-type, multi-pressure design" heat exchanger in which the gas turbine flue gas heat is recovered in triple pressure steam cycles [80]. High pressure (HP), medium/intermediate pressure (IP) and low pressure (LP) steam at respectively pressures of 12.4 MPa/3.1 MPa/0.448 MPa are raised in a series of heat exchangers (see Figure 4.3). The superheated HP steam produced has a temperature of 534ºC and is used for power generation in the HP steam turbine. Simultaneously, IP steam (4.2-4.5MPa) is withdrawn from the HP turbine in order to provide the necessary feed steam for gasification. IP steam consists of the HP turbine outlet and the steam from the HTS product heat recovery. The IP steam is used for process heating and as a feed for WGS, whereas the surplus is reheated to a temperature of 534ºC then charged into an IP steam turbine for additional power generation. Similarly, the LP steam is also used for process heating purposes such as AGR regenerator reboilers while the excess is mixed with the LP steam turbine outlet and sent to the LP steam turbine for power generation. The sulfur recovery process is a heat generating process that is also integrated with the HRSG; however its impact is trivial since it consists of 0.5-1% the total process LP steam.

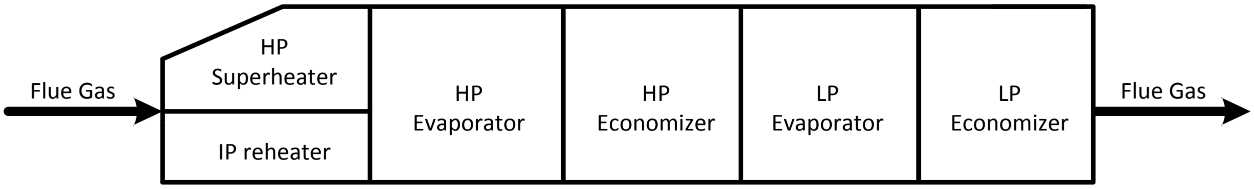

Figure 4.3: Simple BFD of the HRSG flue gas train of heat exchangers

The LP steam turbine outlet and process make-up water are mixed and sent into a deaerator which has to reduce the water dissolved oxygen level to below 7 ppb while eliminating CO_2 traces in order to avoid corrosion problems in the HRSG tubes [137]. The treated water is then split into multiple streams for pumping and reheating. The water is distributed between the HRSG and the process where heat is recovered and re-utilized. It is important to note that process economizers provide the necessary energy for water reheating to around 112.8ºC without requiring any HRSG bleed streams.

The gasification process has an excess of heat and should ideally be energy sufficient. However, the integration of the bitumen upgrading and the gasification process reduces the syngas load intended for the power and steam generation, which decreases the overall efficiency of the IGCC process. Moreover, the percentage of captured CO_2, the conversion of WGS reactors and the gasifier steam requirements can also significantly diminish the process steam load. Therefore, a simulation optimization has to be performed when integrating the IGCC with the bitumen upgrading facility in order to obtain an energy self-sufficient gasification process while producing enough hydrogen for recycle.

4.2.7. Bitumen upgrading process

The simulation of a 100,000 BPD Athabasca bitumen upgrading facility utilizing the Canmet slurry hydrocracking process requires around 1,265 GJ/h of heating fuel, 9,259 m^3/h of cooling water, 321 GJ/h of steam and 71.73 MW of electricity [121]. The process consists of a desalter, diluent recovery unit, vacuum distillation, hydrocracker and three hydrotreaters. The Canmet hydrocracker achieves a residue conversion of 91% while the operation of the hydrotreaters allows an average hydrodesulfurization and hydrodenitrogenation conversion of 90 and 72% for which a total hydrogen consumption of $1.52*10^4$ kg/h is required. The upgrading process produces around 97,000 BPD of synthetic crude oil and emits an estimated 3.997–4.864 million tonne/year of CO_2 depending on the extraction/mining technology employed.

4.3. ***Results and discussion***

The entrained flow slagging gasifier is assumed to reach chemical equilibrium at an operating temperature of 1427ºC [80]. Therefore, the important parameters that impact the gasifier operation are its isothermal temperature and the oxygen and steam feed rates. Figure 4.4 presents case studies during which the hydrogen, carbon monoxide, carbon dioxide, methane and steam generation are monitored in function of various oxygen and steam to carbon ratio. Oxygen-to-carbon ratios should never exceed 0.5 above which complete combustion will start reducing the potential hydrogen yield by burning the CO and producing significantly more CO_2 and steam. Moreover, the process oxygen consumption should also be minimized in order to reduce the costs associate with the ASU. Nevertheless, an oxygen-to-carbon ratio should not be reduced more than 0.4 since it promotes incomplete partial combustion in conjunction with an increase in syngas methane composition and a significant decrease in steam production. If the gasifier were to be operated without steam, the optimal oxygen to carbon ratio would be around 0.5 at which the stoichiometric ratio for partial combustion of the feed carbon content is satisfied. However, coupling oxygen and steam gasification is beneficial as shown in Figure 4.4. The oxygen demand of the gasifier is costly since ASU consume a large amount of energy. Besides, steam addition improves the total potential hydrogen yield, i.e. CO and hydrogen compositions, to over 95% which consequently increases process efficiency and the available upgrading facility recycle hydrogen. An Aspen HYSYS® optimization study established that an oxygen and steam to carbon ratio of 0.421 and 0.159 provided the highest combined hydrogen and CO molar composition without necessitating additional energy for an isothermal operation. On the other hand, in order to maximize the overall process steam production, an oxygen and steam to carbon ratio of 0.45 and 0.1 are chosen. Those operating conditions still provide a potential hydrogen yield exceeding 95% while significantly reducing the steam load of the gasifier and increasing its shell HP steam production.

The most important condition in the integration of the gasification and bitumen upgrading process is to meet the hydrogen demand of the hydrocracker and hydrotreaters obtained at the upgrading base case operated at a 91% hydrocracker residue conversion achieved at a temperature, pressure and LHSV of 450ºC, 18MPa and 0.48 h^{-1}, respectively. The hydrotreaters operating conditions are calibrated in order to reach a 90% and 72% hydrodesulfurization and hydrodenitrogenation conversion. Before implementing the power generation combined cycle to the entrained flow slagging gasifier, the amount of residue feed required to meet upgrading process hydrogen demand has to be determined. At the upgrading base case of 91.2% conversion, the withdrawn hydrocracker residue fed to the gasifier has a flow rate of 29,237 kg/h. If the gasification section were to only operate with the hydrocracker residue feed while keeping all the gasification operating conditions constant, it would produce 3,508kmol/h of

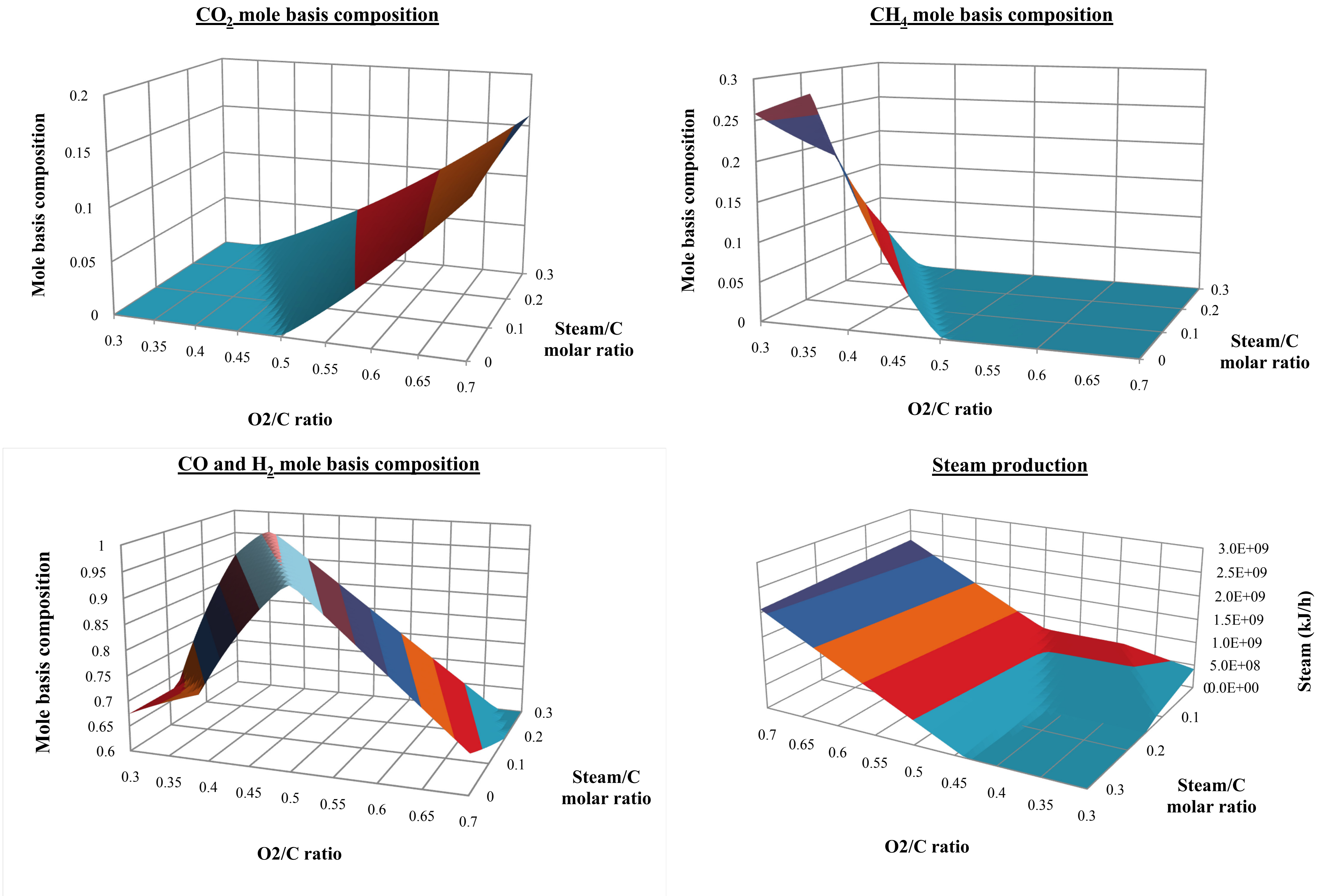
CO_2 mole basis composition

CH_4 mole basis composition

CO and H_2 mole basis composition

Steam production

Figure 4.4: Entrained flow slagging gasifier case studies in function of oxygen and steam to carbon ratios

hydrogen which only meets 46.6% of the plant hydrogen demand. Figure 4.5 presents the relationship between the upgrading hydrogen demand and gasification hydrogen produced in function of hydrocracker conversion based solely on the hydrocracker residue feed. At a residue conversion of 82.4%, the hydrocracker provides the gasifier with enough residue feed to satisfy the upgrading process hydrogen consumption of 7,045kmol/h.

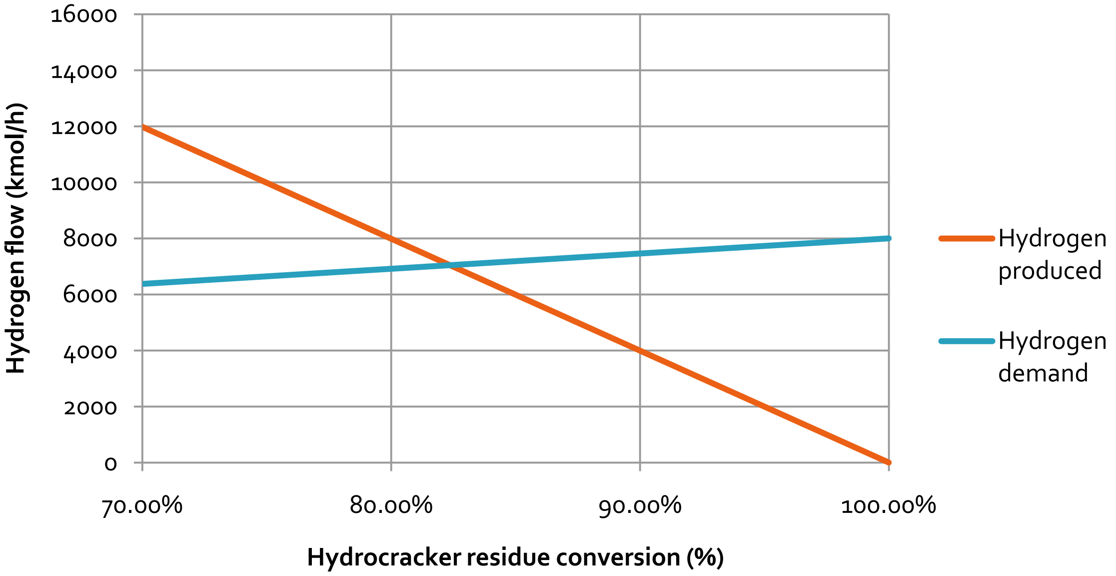

Figure 4.5: Gasifier hydrogen production as a function of hydrocracker residue

Nevertheless, the Canmet slurry hydrocracker cannot be operated at 82.4% conversion since it affects the SCO production and quality. The purpose of the upgrading facility is to obtain a high production yield of quality SCO. Therefore, the residual hydrogen cannot be satisfied by reducing hydrocracker conversion or by by-passing the unit; it has to be produced by other means. The proposed solution consists of processing petroleum coke with the hydrocracker residue gasifier feed in order to increase the syngas throughput. The addition of petroleum coke has a marginal impact on downstream syngas treatment and purification configuration since it consists of a high heteroatom carbonaceous feed, similar to the hydrocracker residue [138]. The

Cold Lake petroleum coke characteristics are available in Table 4.1. If the hydrogen demand of only the upgraders was to be fulfilled, an additional 42,763kg/h of petroleum coke would need to be gasified, which ultimately produces 1.934E+04 Nm^3/h of untreated syngas. For this simulation case, the steam consumption of the gasifier (0.1 steam/C ratio), the WGS reactors (S:DG ratio of 0.25) and the amine regenerator reboiler is satisfied because of the excess heat recovery of the gasification process (see Table 4.5). However, the integrated process will not be electrically self-sufficient since an insufficient quantity of syngas will be remaining for the gas and steam turbine cycle. In order to meet the process electrical requirements, additional petroleum coke has to be gasified for an excess production of syngas that can then be utilized for power generation.

Table 4.5: Energy recovery and requirements of gasification process that satisfies upgrading hydrogen consumption

Heat recovery (kJ/h)

COS hydrolysis humidifiers	4.434E+07
Gasifier shell steam	5.202E+07
Radiant syngas cooler	2.764E+08
HTS recovery	1.486E+08
Syngas humidifier	5.155E+07
Claus heat recovery	1.562E+07
Total	5.886E+08

Steam requirements (kJ/h)

Amine reboiler	2.559E+07
WGS steam	3.621E+08
Gasification cooling section	1.974E+07
Gasifier steam	2.355E+07
Total	4.310E+08

For a power self-sufficient gasification process with 90% CO_2 capture, the gasifier feed has to be increased to 332,000 kg/h of which only 8.8 wt% consists of hydrocracker residue. The flow rate of petroleum coke is thus increased to 302,763 kg/h, a value that is 5.52 times larger than the petroleum coke feed necessary to meet process hydrogen requirement. The excess hydrogen production is necessary to meet the process steam requirement of the MEA process reboiler for pre-combustion carbon capture. The steam consumption of the amine process cannot be satisfied without optimization because the combustion turbine syngas loses a large amount of its heating value when some of its hydrogen content is recycled to the upgrading units. The integrated bitumen upgrading and IGCC operation is self-sufficient in hydrogen, power and steam when a minimum of 76.6% of the hydrogen produced is charged into the gas turbine while 23.4% is recycle. Since LP steam quality is utilized in the reboiler, the operation of LP turbines is futile because of the exhaustion of the LP steam caused by process heating requirements. A total electrical generation of 983MW of which 826MW is attributed to the gas turbine and nitrogen turbo expander and 157MW is generated by the HP/IP steam turbines. The auxiliary power load is presented in Table 4.6 which results in a net plant efficiency on a HHV basis of 29.1%. Compared with the NETL/DOE Shell Global Solutions IGCC Case with 90% carbon capture, the calculated net plant efficiency is lower by around 2% which is caused by the hydrogen recycle withdrawal [80]. Minor auxiliary pumps and compressors were not incorporated in the overall electricity balance but can still be satisfied by the large surplus of residual power. Moreover, hydrogen purification utility consumption with PSA is neglected since the hydrogen composition of the amine CO_2 capture process syngas is over 93mol%.

In order to increase the net plant efficiency, the 90% carbon capture base case is compared with a 65% capture operation. The amount of CO_2 captured is reduced by bypassing the CO_2 amine capture process which scales down the operation consequently lowering the reboiler LP steam consumption. An excess of 17,710kmol/h of steam will be available for power production, increasing the steam turbine power generation to 224MW. The gas turbine and nitrogen expander's power production also increase due to a change in syngas composition. The change in syngas composition requires less nitrogen dilution and allows for a higher overall power generation. As a result, the net plant efficiency increases to 33.1%. Similarly to the 90% capture case, the PSA power consumption is also assumed negligible since syngas exiting the amine CO_2 capture unit is the very rich in hydrogen.

A carbon capture of 65% can also be obtained by bypassing the WGS reactors operated at a constant S:DG ratio. Since the MEA solvent captures CO_2 and H_2S only, the bypassed syngas CO content cannot be sequestrated and should therefore bypass the carbon capture amine process as well. This case will reduce the IP steam consumption of the WGS process and the LP steam consumption of the CO_2 capture process. However, the combustion turbine nitrogen diluent flow rate is not enough to maintain a TIT of 1322ºC hence a HRSG IP steam draw of 17,265kmol/h has to be mixed with the syngas in order to protect the turbine and process equipment while avoiding NO_X formation. As a result, the gas turbine power generation increases due to its higher gas throughput caused by steam dilution whereas the steam turbine power generation diminishes. The TIT could also be controlled by adding a syngas humidifier which raises the water content of the combustion turbine feed and reduces its heat of combustion. The change in net plant efficiency is 0.5% when comparing both 65% carbon capture configurations.

Table 4.6: Overall power generation and consumption of integrated process

Carbon Capture Case	**90%**	**65%**	**65%**	**0%**
Net Plant Efficiency	29.1%	33.1%	33.6%	41.0%
CO_2 amine process bypass	3.9%	31.0%	3.9%	100.0%
WGS process bypass	0.0%	0.0%	27.7%	0.0%
Flue gas CO_2 emissions (million tonne/yr)	0.8752	3.0935	3.0489	8.7492
Total CO_2 emissions (kg/bbl of bitumen)	145.46	206.14	204.92	361.09
CO_2 capture (kg/bbl of bitumen)	215.80	157.40	155.13	0.00

Turbine outlet temperature (ºC)	564.0	571.0	577.4	569.5
Turbine outlet pressure (bar)	1.105	1.105	1.105	1.105

Power generated (MW)

Gas turbine Power	805.99	794.96	914.00	811.94
Nitrogen Expander Power	20.68	41.17	0.00	73.66
Steam Turbine Power	156.74	223.82	168.25	366.77
Total	983.41	1059.95	1082.25	1252.37

Auxiliary power load (MW)

Oxygen Compressors	16.76	16.76	16.76	16.76
Nitrogen Compressors	69.45	69.45	69.45	69.45
ASU Air Compressors	127.54	127.54	127.54	127.54
CO_2 Compression	75.79	54.37	54.39	0.00
CO_2 Removal Power	25.00	17.92	17.97	0.00
H_2S Removal Power	1.37	1.37	1.37	1.37
Upgrading Process	71.73	71.73	71.73	71.73
Condensate Water Pumps	2.25	2.46	2.23	2.57
Syngas Recycle	3.62	3.62	3.62	3.62
Pressure Swing Adsorption	0.00	0.00	0.00	12.26
Total	393.51	365.22	365.06	305.30

Finally, when the CO_2 removal section is completely disconnected resulting in a gasification operation with no carbon capture, the net plant efficiency increases to 41.0% since all the LP steam is utilized for power generation instead of rich solvent regeneration. The WGS section is however not by-passed during the zero carbon capture case in order to maintain the syngas composition within the scope of the chosen gas turbine. Also, the necessary recycle hydrogen requires a PSA hydrogen separation since it is diluted. The PSA process concentrates the hydrogen steam to 99+% while mixing back the residual syngas stream with the gas turbine syngas. The power consumption of the PSA process is found to be around 60kW/1000Nm^3 of hydrogen-free syngas [139, 140].

When 90% of the carbon is captured in the gasification process, the process CO_2 emissions are reduced to 0.8752 million tonne per year. For the 65% carbon and no carbon capture cases, the emissions increase to around 3.05 and 8.75 million tonne per year respectively, compared to the 3.997–4.864 million tonne per year of CO_2 for the extraction/mining and upgrading of the 100,000 BBD of Athabasca bitumen [121]. Thus, the addition CO_2 capture technology to the gasification process allows the integrated facilities to capture around 60% for the 90% capture case and 43% for the 65% capture case. Furthermore, the integrated processes emit around 145 kg CO_2 per barrel of bitumen for the 90% capture case, 205 kg/bbl for the 65% capture case and 361 kg/bbl for no CO_2 capture.

In order to meet the upgrading hydrogen demand and the gasification process energy requirements, the proposed upgrading process needs to produce 983 MW of power by consuming a carbonaceous feed that is about 1.6 times larger than the IGCC cases studied by NETL/DOE [80]. The utilization of the hydrocracking upgrading technology is still justifiable relative to thermal upgrading technologies, which diminish the hydrogen consumption of the upgrading process but also reduce SCO production. Alternatively, various gasification process alterations can help reduce the plant size. For example, different carbon capture technologies can be tested. PSA is an electrical consuming technology which can benefit from the gasification process power surplus. Also, CO_2 capture by calcium looping is being researched at the Canmet facility and can be implemented and evaluated against other technologies, e.g. Rectisol, Selexol, Sulfinol and MDEA in the integrated simulation context. For the case of obtaining a self-sustainable process, the objective of testing various CO_2 technologies is not to optimize the carbon capture efficiency but to minimize the LP steam consumption, a process utility that is limited because of the upgrading process hydrogen extraction. Nonetheless, the operation of a self-sustainable process might not be the most economical. The operation of various capture technologies might provide self-sufficiency but reduce the overall profit of the process due to excessive operation costs. An economic analysis could be performed in order to compare the profitability of the various potential process layouts. Furthermore, a process configuration that potentially reduces the facility size is replacing the sweet WGS reactors with their sour WGS counterpart. The sweet WGS has the advantage of operating at a higher temperature than the sour process which reduces the process overall irreversible heat loss [78]. However, due to the sensitivity of the catalyst to sulfur, it is necessary to treat the syngas in an AGR section before the HTS reactor. If the sour WGS process were to be implemented, the syngas treatment process can all be performed at the pre-combustion stage during a selective AGR for the CO_2 and H_2S removal. Moreover, the cold amine gas cleanup process preceding sweet WGS condenses a significant amount of water vapour present in the syngas which results in an efficiency loss caused by the increase of the WGS IP steam feed.

4.4. ***Conclusion***

A gasification process with carbon capture is simulated and integrated with a bitumen upgrading facility in order to obtain a hydrogen, power and energy self-sufficient operation. An entrained flow slagging gasifier is chosen for the gasification of the hydrocracker petroleum feed at an oxygen and steam to carbon molar ratio of 0.45 and 0.1. Only 34.8% of the hydrogen demand of the hydrocracker operating at a conversion of 91% and constant hydrodesulfurization and hydrodenitrogenation of 90% and 72% for the hydrotreaters is satisfied if the hydrocracker residue alone is gasified. A reduction in hydrocracker conversion or a vacuum residue by-pass is not beneficial since it reduces the SCO yield. Therefore, a petroleum coke addition of 42,763kg/h is necessary in order to meet the 7525kmol/h of hydrogen required by the upgrading section. In order to implement carbon capture and supply the process with power via the integration of gas and steam turbines, a larger quantity of petroleum coke has to be charged into the gasifier in order to produce excess syngas that can be used for power and steam generation. A 90% carbon capture gasification process that is self-sufficient in power and heat and meets the required recycle hydrogen demand requires the addition of 302,763 kg/h of petroleum coke. The gas and steam turbines produce a total of 983MW with a net plant efficiency of 29.1% while capturing 216 kg CO_2 per barrel of bitumen upgraded. If the extent carbon capture were to be reduced to 65%, the net plant efficiency increases to over 33.1% producing 1,060MW of power and capturing 156 kg CO_2 per barrel of oil. For a no carbon capture case, a carbon emission of 13.2 million tonne of CO_2 per year is released for the extraction and upgrading of 100,000 BBD of bitumen integrated with a gasification process. The power generated by the process increases to 1252MW with a net plant efficiency of 41%. For the 65% carbon capture case, a by-pass of the WGS and amine process resulted in slightly higher net plant efficiencies but required the addition of steam and nitrogen to the combustion turbine, in order to control the flame temperature. The plant efficiency can be raised further by replacing the chosen WGS technology with its sour counterpart. Also, the MEA carbon capture process utilizes a significant amount of LP steam which necessitates the gasification process to be about 1.6 times larger than the IGCC cases studied by NETL/DOE. Therefore, testing various carbon capture technologies for the reduction of process steam utilization can help reduce the plant size required to meet the recycle hydrogen, power and heating demand of the integrated process for the base case of 90% carbon capture.

5. Conclusion and recommendations

The integration of the bitumen upgrading facility and the gasification process with 90% carbon capture is technically feasible for a production of 97,000 BPD of SCO with a density of 27.71ºC and a heteroatom content of 0.164wt% sulfur and 0.066wt% nitrogen. The gasification process steam requirements and upgrading process hydrogen and power demand are satisfied in the integrated simulation when the hydrocracker is operated at 91% conversion. A gasifier feed of 332,000kg/h is also necessary for a net power generation of 589.9MW. The total amount of CO_2 emitted for a 90% IGCC carbon capture case is 145.5 kg CO_2 per barrel of SCO produced. The integrated MEA carbon capture process necessitates a gasification process that is 1.6 times larger than the IGCC cases evaluated by NETL/DOE [80]. However, for a lower carbon capture percentage, the necessary gasifier feed can be reduced due to the lower LP steam process requirements.

As a result of the analysis and objectives pursued in this thesis, the following recommendations could lead to the improvement of the integrated process and the optimization of many of the utilized technologies:

- The proposed Canmet slurry hydrocracker hybrid model can be improved if more data regarding the petroleum product mass fraction distribution, the sulfur and nitrogen content of the product and light end distribution for the slurry hydrocracking of vacuum residue (b.p. 540+ºC) with a low-activity catalyst/additive were provided. Consequently, a more complete kinetic model can be developed in order to calculate the extent of hydrocracking and hydrotreating and the petroleum product distribution and elemental composition.

- The hydrocracker and hydrotreater simulation could be improved if specific operating data were obtained regarding the hydrogen consumption, hydrogen recycle, utility requirements, etc.
- The addition of the hydrodearomatization reaction to the calibration parameters of the naphtha, light gas oil and heavy gas oil hydrotreaters and to the hydrocracker model can allow the simulation to accurately characterize the aromatic fraction in the SCO product. Similarly to API density and heteroatom content, the aromatic content of the SCO affects the quality of the fuel.
- The sweet WGS technology can be replaced with a sour WGS configuration which consequently permits the omission of the amine process intended for sulfur removal. As a result, the removal of CO_2 and H_2S can be combined into one selective pre-combustion acid gas removal process.
- Various carbon capture technologies could be tested in order to optimize the net plant efficiency and the steam cycle of the gasification process. Various chemical and physical absorption processes, e.g. an MDEA, Rectisol, Selexol or Sulfinol process, a pressure swing adsorption process or a calcium looping process could be simulated to replace the proposed AGR MEA solvent.
- An economical study is necessary for comparing the different potential plant layouts. The addition of capital and operating costs allows for the optimization of the process in function of the varying market prices of natural gas, coal, oil, electricity and carbon dioxide for potential future applications.

6. References

1. *World Energy Outlook*. 2009, International Energy Agency: London.

2. Castañeda, L.C., J.A.D. Muñoz, and J. Ancheyta, *Combined process schemes for upgrading of heavy petroleum.* Fuel, 2012.

3. Scherzer, J. and A.J. Gruia, *Hydrocracking Science and Technology*, ed. M. Dekker. 1996, New York: Marcel Dekker.

4. Ancheyta, J. and J.G. Speight, *Hydroprocessing of heavy oils and residua*. 2007: CRC Press.

5. Fahim, M.A., T.A. Al-Sahhaf, and A. Elkilani, *Fundamentals of Petroleum Refining*. 2010: Elsevier.

6. Furimsky, E., *Catalysts for upgrading heavy petroleum feeds*. 2007: Elsevier.

7. Gary, J.H.a.H., G. E. -, *Petroleum Refining - Technology and Economics*. 5 ed. 2001, New York: Marcel Dekker Inc.

8. Gray, M., *Hydrocarbon Fluid Properties and Processing*. 2006, Alberta: Department of Chemical and Material Engineering.

9. Speight, J.G., *The desulfurization of heavy oils and residua*. 1981: M. Dekker.

10. Speight, J.G. and B. Ozum, *Petroleum Refining Processes*. Marcel Dekker ed. 2002, New York: Marcel Dekker.

11. Wiehe, I.A., *Process Chemistry of Petroleum Macromolecules*, ed. J.G. Speight. 2008, Berkeley, California: Chemical Industries.

12. Basak, K., et al., *Industrial hydrocracker model based on novel continuum lumping approach for optimization in petroleum refinery.* Catalysis Today, 2004. **98**(1-2): p. 253-264.

13. Ashuri, E., F. Khorasheh, and M.R. Gray, *Development of a continuous kinetic model for catalytic hydrodenitrogenation of bitumen.* Scientia Iranica, 2007. **14**(2): p. 152-160.

14. Harris, K., et al., *Field Experience with a single NDUV & TCD Analyser on Amine-Based Tail Gas Treatment Units*, in *ISA 52nd Analysis Division Symposium*, AMATEK, Editor. 2007: Houston, TX.

15. Abraham, H., *Asphalts and allied substances, their occurrence, modes of production, uses in the Arts, and methods of testing: Methods of testing:industrial raw bituminous materials*. 1962: Van Nostrand.

16. Citizendium. *Hydrocracking*. 2011 [cited 2011; Available from: http://en.citizendium.org/wiki/Hydrocracking.

17. FactSage. *Hydrocracking Residue Three-Phase Diagram*. 2011 [cited 2011; Available from: http://www.factsage.com/.

18. MetalPrices. *Metal commodity prices*. 2011 [cited 2011; Available from: http://www.metalprices.com/.

19. Balasubramanian, P. and S. Pushpavanam, *Model discrimination in hydrocracking of vacuum gas oil using discrete lumped kinetics.* Fuel, 2008. **87**(8-9): p. 1660-1672.

20. Alvarez, A. and J. Ancheyta, *Modeling residue hydroprocessing in a multi-fixed-bed reactor system.* Applied Catalysis A: General, 2008. **351**(2): p. 148-158.

21. Bower, T., *Oil: Money, Politics, and Power in the 21st Century*. 2010: Grand Central Publishing.

22. Pacheco, M.A. and C.G. Dassori, *Hydrocracking: An improved Kinetic Model and Reactor Modeling.* Chemical Engineering Communications, 2002. **189**(12): p. 1684 - 1704.

23. Ancheyta, J., S. Sánchez, and M.A. Rodríguez, *Kinetic modeling of hydrocracking of heavy oil fractions: A review.* Catalysis Today, 2005. **109**(1-4): p. 76-92.

24. Koscielnuk, D., et al., *Low Cost and Reliable Sulfur Recovery*, J.C.S. Solutions and MECS, Editors.

25. Basini, L., *Issues in H2 and synthesis gas technologies for refinery, GTL and small and distributed industrial needs.* Catalysis Today, 2005. **106**(1–4): p. 34-40.

26. *International Energy Statistics*. U.S. Energy Information Administration 2012; Available from: http://www.eia.gov/cfapps/ipdbproject/IEDIndex3.cfm.

27. Duchesne, M., *Slagging in Entrained-Flow Gasifiers*, in *Chemical and Biological Engineering*. 2012, University of Ottawa: Ottawa.

28. Duchesne, M., et al., *Optimization of Canadian petroleum coke, coal and fluxing agent blends via slag viscosity measurements and models*, in *International Pittsburgh Coal Conference*. 2010, Pittsburgh Coal Conference: Istanbul, Turkey. p. 14.

29. Rettger, P., et al., *The Long Lake Integrated Upgrading Project: Status report and discussion on soot processing*. 2006. p. 9.

30. Schlichting, H., S. Walter, and J. Quinn. *Hydrogen production by MPG-Gasification for upgrading Canadian oil sands*. in *2nd International Freiberg Conference on IGCC & XTL Technologies*. 2007. Frieberg.

31. Shell, *Cutting deeper into the barrel*, in http://www-static.shell.com/static/globalsolutions/downloads/aboutshell/key_projects/case_study_pernis.pdf, Shell, Editor. 2008, Shell.

32. Bruce, G., *From wells to wheels.* Heavy Oil & Oil Sands, 2008. **3**(Guidebook and directory): p. 147-150.

33. Strausz, O.P., E.M. Lown, and A.E.R. Institute, *The Chemistry of Alberta Oil Sands, Bitumens and Heavy Oils*. 2003: Alberta Energy Research Institute.

34. Laboratories, J.E. *SARA - Saturates, Aromatics, Resins and Asphaltenes*. 2006 [cited 2011 15-01-2011]; Available from: http://www.jones-forensics.com/technical-information/sara-analysis.aspx.

35. de Almeida, R.M. and R. Guirardello, *Hydroconversion kinetics of Marlim vacuum residue.* Catalysis Today, 2005. **109**(1-4): p. 104-111.

36. Sadighi, S., A. Ahmad, and S.R. Seif Mohaddecy, *6-lump kinetic model for a commercial vacuum gas oil hydrocracker.* International Journal of Chemical Reactor Engineering, 2010. **8**.

37. Pedersen, K.S., A. Fredenslund, and P. Thomassen, *Properties of oils and natural gases*. 1989: Gulf Pub. Co., Book Division.

38. Twu, C.H., *Internally consistent correlation for predicting liquid viscosities of petroleum fractions.* Industrial & Engineering Chemistry Process Design and Development, 1985. **24**(4): p. 1287-1293.

39. Petheram, L., *Acid Rain*. 2002: Bridgestone Books.

40. Nelson, W.L., *Petroleum refinery engineering*. 1958: McGraw-Hill.

41. Gruse, W.A. and D.R. Stevens, *The Chemical Technology of Petroleum...: By William A. Gruse and Donald R. Stevens... 2nd Edition*. 1942: McGraw-Hill book Company.

42. Speight, J.G., *The Chemistry And Technology of Petroleum*. 2007: CRC Press/Taylor & Francis.

43. *Aspen HYSYS®*. 2012 [cited 2010-2012; Available from: http://www.aspentech.com/hysys/.

44. Bhattacharyya, D., R. Turton, and S.E. Zitney, *Steady-State Simulation and Optimization of an Integrated Gasification Combined Cycle Power Plant with CO2 Capture.* Industrial & Engineering Chemistry Research, 2010. **50**(3): p. 1674-1690.

45. *Customization Guide*, I. Aspen Technology, Editor. 2010, Aspen Technology, Inc.

46. *Thermodynamics COM Interface*, I. Aspen Technology, Editor. 2010, Aspen Technology, Inc.

47. *Aspen HYSYS-OLI Interface*, I. Aspen Technology, Editor. 2010, Aspen Technology, Inc.

48. *Aspen HYSYS Refining - Operations Guide*, I. Aspen Technology, Editor. 2010, Aspen Technology, Inc.

49. Rezaiyan, J. and N.P. Cheremisinoff, *Gasification technologies: a primer for engineers and scientists*. 2005: Taylor & Francis.

50. Higman, C. and M. Burgt, *Gasification*. 2003: Elsevier/Gulf Professional Pub.

51. Baker, M.D., *Gasification: Chemistry, Processes and Applications*. 2011: Nova Science Pub Incorporated.

52. Sudiro, M., et al., *Dual-Bed Gasification of Petcoke: Model Development and Validation.* Energy & Fuels, 2010. **24**(2): p. 1213-1221.

53. Nathen, S.V., R.D. Kirkpatrick, and B.R. Young, *Gasification of New Zealand Coals: A Comparative Simulation Study.* Energy & Fuels, 2008. **22**(4): p. 2687-2692.

54. Descamps, C., C. Bouallou, and M. Kanniche, *Efficiency of an Integrated Gasification Combined Cycle (IGCC) power plant including CO2 removal.* Energy, 2008. **33**(6): p. 874-881.

55. Nikoo, M.B. and N. Mahinpey, *Simulation of biomass gasification in fluidized bed reactor using ASPEN PLUS.* Biomass and Bioenergy, 2008. **32**(12): p. 1245-1254.

56. Munteanu, M.C. and J. Chen. *Optimizing Bitumen Upgrading Scheme - Modeling and Simulation Approach*. in *2012 AIChE Spring Meeting*. 2012. Houston, TX.

57. Wang, J., et al., *Properties correlations and characterization of Athabasca oil sands-derived synthetic crude oil.* Petroleum Science, 2007. **4**(3): p. 84-90.

58. Yang, C., et al., *Alumping kinetic model of residuum hydrocracking.* Acta Petrolei Sinica (Petroleum Processing Section), 1999. **15**(5): p. x8-49.

59. Drago, G., J. Gultian, and J. Krasuk, *The development of HDH process, a refiners tool for redidual upgrading.* American Chemical Society, 1990. **Division of Fuel Chemistry**(35): p. 584-592.

60. Zhang, S., et al., *A Review of Slurry-Phase Hydrocracking Heavy Oil Technology.* Energy & Fuels, 2007. **21**(6): p. 3057-3062.

61. Mederos, F.S., J. Ancheyta, and J. Chen, *Review on criteria to ensure ideal behaviors in trickle-bed reactors.* Applied Catalysis A: General, 2009. **355**(1-2): p. 1-19.

62. Panariti, N., et al., *Petroleum residue upgrading with dispersed catalysts: Part 1. Catalysts activity and selectivity.* Applied Catalysis A: General, 2000. **204**(2): p. 203-213.

63. Denis, J.M., K. Belinko, and B.N. Nandi, *Analysis of reactor samples collected during thermal hydrocracking of Athabasca Bitumen.* CANMET Report (Canada Centre for Mineral and Energy Technology), 1976(77-51).

64. Prasad, R., et al., *A Methodology for Screening Hydrocracking Catalysts.* J. Chem. Tech. Biotechnol, 1995(64): p. 195-199.

65. Vazquez, M.I., A. Escardino, and A. Aucejo, *Hydrocracking of n-heptane with a nickel monoxide-molybdenum trioxide/HY ultrastable zeolite as catalyst. The network of the reaction.* Industrial & Engineering Chemistry Research, 1988. **27**(11): p. 2039-2043.

66. Baltanas, M.A., H. Vansina, and G.F. Froment, *Hydroisomerization and hydrocracking. 5. Kinetic analysis of rate data for n-octane.* Industrial & Engineering Chemistry Product Research and Development, 1983. **22**(4): p. 531-539.

67. Froment, G.F., *Kinetics of the hydroisomerization and hydrocracking of paraffins on a platinum containing bifunctional Y-zeolite.* Catalysis Today, 1987. **1**(4): p. 455-473.

68. Steijns, M. and G.F. Froment, *Hydroisomerization and hydrocracking. 3. Kinetic analysis of rate data for n-decane and n-dodecane.* Industrial & Engineering Chemistry Product Research and Development, 1981. **20**(4): p. 660-668.

69. Roussel, M., et al., *Hydrocracking of n-decane on a bifunctional sulfided NiW/silica-alumina catalyst: effect of the operating conditions.* Applied Catalysis A: General, 2005. **279**(1-2): p. 53-58.

70. Svoboda, G.D., et al., *Single-Event Rate Parameters for Paraffin Hydrocracking on a Pt/US-Y Zeolite.* Industrial & Engineering Chemistry Research, 1995. **34**(11): p. 3793-3800.

71. Gillis, D., M. VanWees, and P. Zimmerman, *Upgrading residues to maximize distillate yields* A.H.C. UOP LLC, Editor. 2009: Des Plaines, Illinois, U.S.A.

72. Patmore, D.J. and B.B. Pruden, *Thermal hydrocracking of Athabasca Bitumen : Comparison of computer simulated values of feed and product vaporization with CANMET pilot plant data.* CANMET Report (Canada Centre for Mineral and Energy Technology), 1980(80-23E).

73. Patmore, D.J., A.M. Shah, and B.B. Pruden, *THERMAL HYDROCRACKING OF ATHABASCA BITUMEN: COMPUTER SIMULATION OF FEED AND PRODUCT VAPORIZATION.* CANMET Rep, 1977(78-4).

74. Pruden, B.B., J.M. Denis, and A.M. Shah, *Thermal hydrocracking of Athabasca Bitumen: Steady-state effects of product yields and qualities in absence of scrubbing of the recycle gas.* CANMET Rep, 1976(77-44).

75. Pruden, B.B., *Hydrocracking of bitumen and heavy oils at CANMET.* The Canadian Journal of Chemical Engineering, 1978. **56**(3): p. 277-280.

76. Morawski, I. and J. Mosio-Mosiewski, *Effects of parameters in Ni–Mo catalysed hydrocracking of vacuum residue on composition and quality of obtained products.* Fuel Processing Technology, 2006. **87**(7): p. 659-669.

77. Bell, D.A., B.F. Towler, and M. Fan, *Coal Gasification and Its Applications*. 2010: Elsevier.

78. Grol, E., *Evaluation of Alternate Water Gas Shift Configurations for IGCC Systems*, in *Bituminous Coal and Natural Gas to Electricity*. 2009, DOE/NETL. p. 32.

79. Porocel. *Activated Aluminas*. [cited 2012; Available from: http://www.porocel.com/34-activated_aluminas/.

80. Haslbeck, J.L., et al., *Cost and Performance Baseline for Fossil Energy Plants*, in *Bituminous Coal and Natural Gas to Electricity*, DOE/NETL, Editor. 2010.

81. Kohl, A.L. and R.B. Nielsen, *Gas purification*. 1997: Gulf Pub.

82. Rao, A.B. and E.S. Rubin, *A Technical, Economic, and Environmental Assessment of Amine-Based CO2 Capture Technology for Power Plant Greenhouse Gas Control.* Environmental Science & Technology, 2002. **36**(20): p. 4467-4475.

83. *Engineering Data Book SI Version*, ed. G.P. Association. Vol. 2. 1998: Gas Processors Suppliers Association.

84. Polasek, J. and J.A. Bullin, *Selecting Amines for Sweetening Units*, I. Bryan Research & Engineering, Editor. 2006, Bryan Research & Engineering, Inc. and Department of Chemical Engineering, Texas A&M University.

85. Shao, R. and A. Stangeland, *Amines Used in CO2 Capture*, Bellona, Editor. 2009, The Bellona Foundation.

86. Wong, S., *CO2 Compression and Transportation to Storage Site*, in *Building Capacity for CO2 Capture and Storage in the APEC region: A training manual for policy makers and practitioners*. 2009, Asia-Pacific Economic Cooperation.

87. Kanniche, M. and C. Bouallou, *CO2 capture study in advanced integrated gasification combined cycle.* Applied Thermal Engineering, 2007. **27**(16): p. 2693-2702.

88. Rameshni, M. and R. Street, *PROClaus: The New Standard for Claus Performance*. 2001, WorleyParsons.

89. Street, R. and M. Rameshni, *Sulfur Recovery Unit: Expansion Case Studies*, WorleyParsons, Editor, WorleyParsons.

90. Davenport, W.G. and M.J. King, *Sulfuric acid manufacture: analysis, control and optimization*. 2006: Elsevier.

91. *World Energy Outlook*. 2008, International Energy Agency.

92. Robinson, P.R. and G.E. Dolbear, *Hydrotreating and hydrocracking: fundamentals*. Practical advances in petroleum processing, ed. P.R.R. C.S. Hsu. Vol. 1. 2006, New York Springer.

93. Inc., N. *How Long Lake Works*. 2012; Available from: http://www.nexeninc.com/en/Operations/OilSands/HowLongLakeWorks.aspx.

94. Aiello, J., S. Walter, and J. Quinn. *North West Upgrader with Lurgi MPG for Hydrogen Production*. in *Processing Canadian Oil sands & Coal Using Gasification*. 2007. Calgary, Canada.

95. *Opportunities and Challenges to 2015 - An Energy Market Assessment*. 2004, National Energy Board.

96. Polyzakis, A.L., C. Koroneos, and G. Xydis, *Optimum gas turbine cycle for combined cycle power plant.* Energy Conversion and Management, 2008. **49**(4): p. 551-563.

97. Netzer, D., *Alberta Bitumen Processing Integration Study.* The Alberta Energy Research Institute, 2006: p. 164.

98. aspentech. *Aspen HYSYS Property Packages: Overview and Best Practices for Optimum Simulations*. in *Aspen Process Engineering Webinar*. 2006.

99. Parkash, S., *Refining Process Handbook*, ed. Elsevier. 2003: Gulf Professional Publishing. 712.

100. Puttagunata, V.R., B. Singh, and A. Miadonye, *Correlation of bitumen viscosity with temperature and pressure.* The Canadian Journal of Chemical Engineering, 1993. **71**(3): p. 447-450.

101. Dan Gillis, M.V., Paul Zimmerman, *Upgrading Residue to Maximum Distillate Yields*. 2009, UOP: Des Plaines, Illinois, USA.

102. Köseoḡlu, R.Ö. and C.R. Phillips, *Kinetic models for the non-catalytic hydrocracking of Athabasca bitumen.* Fuel, 1988. **67**(7): p. 906-915.

103. Yui, S.M. and E.C. Sanford, *Mild hydrocracking of bitumen-derived coker and hydrocracker heavy gas oils: kinetics, product yields, and product properties.* Industrial & Engineering Chemistry Research, 1989. **28**(9): p. 1278-1284.

104. Sadighi, S., A. Ahmad, and M. Rashidzadeh, *4-Lump kinetic model for vacuum gas oil hydrocracker involving hydrogen consumption.* Korean Journal of Chemical Engineering, 2010. **27**(4): p. 1099-1108.

105. Laxminarasimhan, C.S., R.P. Verma, and P.A. Ramachandran, *Continuous Lumping Model for Simulation of Hydrocracking.* AIChE Journal, 1996. **42**(9): p. 2645-2653.

106. Fukuyama, H. and S. Terai, *Kinetic Study on the Hydrocracking Reaction of Vacuum Residue Using a Lumping Model.* Petroleum Science and Technology, 2007. **25**(1): p. 277 - 287.

107. Perego, C. and S. Peratello, *Experimental methods in catalytic kinetics.* Catalysis Today, 1999. **52**(2–3): p. 133-145.

108. Carbonell, M.M. and R. Guirardello, *Modelling of a slurry bubble column reactor applied to the hydroconversion of heavy oils.* Chemical Engineering Science, 1997. **52**(21–22): p. 4179-4185.

109. Shah, A.M., B.B. Pruden, and J.M. Denis, *Thermal hydrocracking of Athabasca Bitumen: Correlation of reactor voidage in vertical two-phase flow.* CANMET Rep, 1976(77-44).

110. Koyama, H., et al., *Commercial experience in vacuum residue hydrodesulfurization*, in *Studies in Surface Science and Catalysis*, J.B. M. Absi-Halabi and A. Stanislaus, Editors. 1996, Elsevier. p. 147-155.

111. Fixari, B., et al., *New Developments in Deep Hydroconversion of Heavy Oil Residues with Dispersed Catalysts. 1. Effect of Metals and Experimental Conditions.* Energy & Fuels, 1994. **8**(3): p. 588-592.

112. Martínez, J., et al., *A Review of Process Aspects and Modeling of Ebullated Bed Reactors for Hydrocracking of Heavy Oils.* Catalysis Reviews, 2010. **52**(1): p. 60-105.

113. Magee, J.S. and G.E. Dolbear, *Petroleum Catalysis in Nontechnical Language*. 1998: PennWell.

114. *Annual Report: Oil Sands*. 2011, Nexen Inc.

115. Lupien, T. and F.W. Wu, *Diagnosing and Correcting a Rub in a Mechanical Drive Steam Turbine at Syncrude Canada*. 2007.

116. Vartivarian, D. and H. Andrawis, *Delayed coking schemes are most economical for heavy-oil upgrading.* Oil and Gas Journal, 2006. **104**(6): p. 52-56.

117. Charpentier, A.D., J.A. Bergerson, and H.L. MacLean, *Understanding the Canadian oil sands industry's greenhouse gas emissions.* Environmental Research Letters, 2009. **4**(1).

118. Bergerson, J.A., et al., *Life Cycle Greenhouse Gas Emissions of Current Oil Sands Technologies: Surface Mining and In Situ Applications.* Environmental Science & Technology, 2012. **46**(14): p. 7865-7874.

119. Furimsky, E., *Emissions of Carbon Dioxide from Tar Sands Plants in Canada.* Energy and Fuels, 2003. **17**(6): p. 1541-1548.

120. Herron, H., *Tar Sands as a U.S. Energy Resource*. 2011, Petroleum Equities Inc.

121. Gemayel, J.E., *Integration and simulation of a bitumen upgrading facility and an IGCC process with carbon capture*, in *Chemical and Biological Engineering*. 2012, University of Ottawa: Ottawa.

122. DOE/NETL. *Gasifipedia: Supporting Technologies (Air Separation)*. 2012; Available from: http://www.netl.doe.gov/technologies/coalpower/gasification/gasifipedia/5-support/5-2_airseparation.html.

123. Lurgi. *The Rectisol® Process*. 2010 [cited 2010 March 10th]; Available from: http://www.lurgi.com/website/fileadmin/user_upload/1_PDF/1_Broshures_Flyer/englisch/0308e_Rectisol.pdf.

124. Govind, R. and J. Shah, *Modeling and simulation of an entrained flow coal gasifier.* AIChE Journal, 1984. **30**(1): p. 79-92.

125. Liu, G.S., et al., *Modelling of a pressurised entrained flow coal gasifier: the effect of reaction kinetics and char structure.* Fuel, 2000. **79**(14): p. 1767-1779.

126. Furimsky, E., *Gasification of oil sand coke: Review.* Fuel Processing Technology, 1998. **56**(3): p. 263-290.

127. Shannon, G.N., et al., *Effect of size and density on the thermodynamic predictions of coal particle phase formation during coal gasification.* Fuel Processing Technology, 2009. **90**(9): p. 1114-1121.

128. Chiesa, P., et al., *Co-production of hydrogen, electricity and CO2 from coal with commercially ready technology. Part A: Performance and emissions.* International Journal of Hydrogen Energy, 2005. **30**(7): p. 747-767.

129. Kovacik, G., et al., *Equilibrium calculations in coal gasification.* International Journal of Hydrogen Energy, 1990. **15**(2): p. 125-131.

130. Øi, L.E., *Aspen HYSYS Simulation of CO2 Removal by Amine Absorption from a Gas Based Power Plant*, in *The 48th Scandinavian Conference on Simulation and Modeling (SIMS 2007), 30-31 October, 2007, Göteborg (Särö)*. 2007, Linköping University Electronic Press, Linköpings universitet. p. 73-81.

131. Rao, A., A. Verma, and D.H. Cortez. *Optimization of the shift conversion unit in a gasification plant*. in *Gasification Technologies Council*. 2006. Washington DC.

132. Choi, Y. and H.G. Stenger, *Water gas shift reaction kinetics and reactor modeling for fuel cell grade hydrogen.* Journal of Power Sources, 2003. **124**(2): p. 432-439.

133. Dugstad, T. and E.T. Jensen, *CO2 Capture from Coal fired Power Plants*, in *Department of Energy and Process Engineering*. 2008, Norwegian University of Science and Technology.

134. GEI-41040G, *Specification for Fuel Gases for Combustion in Heavy-Duty Gas Turbines*, in *GE Power Systems*. 2002.

135. Emun, F., et al., *Integrated gasification combined cycle (IGCC) process simulation and optimization.* Computers & Chemical Engineering, 2010. **34**(3): p. 331-338.

136. Chase, D.L. and P.T. Kehoe, *GE Combined-Cycle Product Line and Performance*, in *GER-3574G*, G.P. Systems, Editor, GE Power Systems.

137. Company, S.D. *The Deaerator Principle*. [cited 2012; Available from: http://www.sterlingdeaerator.com/D_Prin.html.

138. Nourouzi-Lavasani, S., F. Larachi, and M. Benali, *Energy and Hydrogen Coproduction from (Athabasca Bitumen) Coke Gasification with CO2 Capture.* Industrial & Engineering Chemistry Research, 2008. **47**(18): p. 7118-7129.

139. SEPMEM. *Gas Separation by PSA*. [cited 2012; Available from: http://www.sepmem.com/products_en.asp?caid=1.

140. *Hydrogen Recovery by Pressure Swing Adsorption*, L. AG, Editor, Engineering Division.